

<https://doi.org/10.1038/s41699-024-00522-4>

Advancements in 2D layered material memristors: unleashing their potential beyond memory

Check for updates

Kiran A. Nirmal^{1,5}, Dhananjay D. Kumbhar^{2,5}, Arul Varman Kesavan³, Tukaram D. Dongale^{2,4} ✉ & Tae Geun Kim^{1,4} ✉

The scalability of two-dimensional (2D) materials down to a single monolayer offers exciting prospects for high-speed, energy-efficient, scalable memristors. This review highlights the development of 2D material-based memristors and potential applications beyond memory, including neuromorphic, in-memory, in-sensor, and complex computing. This review also encompasses potential challenges and future opportunities for advancing these materials and technologies, underscoring the transformative impact of 2D memristors on versatile and sustainable electronic devices and systems.

In 1971, Professor Leon Chua theoretically predicted the existence of a memristor from the symmetry arguments, sparking significant efforts to realize it as an electronic device¹. However, the memristor concept only received limited attention in the late 20th century. Although theoretical discussions continue in academic circles, there has been no significant experimental progress or practical implementation due to technological limitations. In 2008, Strukov et al. from Hewlett-Packard (HP) laboratory successfully demonstrated memristive behavior in a device using a Pt/TiO₂/Pt structure, which was the pioneering paper on memristors². The behavior the authors described is initiated by the migration of oxygen vacancies through the switching layer. Significant advancements in the understanding and development of memristors occurred after 2010. Various research groups worldwide have started experimenting with different materials and configurations for memristors, exploring their potential for use in non-volatile memory (NVM), logic circuits, and neuromorphic computing. Furthermore, HP Labs demonstrated memristors' use in logic operations, demonstrating their potential to go beyond memory applications and function as components in a new type of computing architecture³. The global memristor market is projected to increase by over 80% in 2024 and reach USD 13.5 billion by 2027⁴. Global companies are driving this growth, with many headquartered in the US and EU making significant R&D investments⁵. Memristors are increasingly being perceived as crucial components for building neuromorphic systems that mimic the human brain's neural networks⁶. Moreover, the unique properties of memristors, such as their ability to store and process information simultaneously, are being leveraged to enhance artificial intelligence (AI) and machine learning (ML) algorithms^{7,8}.

Memory technology has become critical in the current era of big data and high-speed information, especially in AI applications. The digital universe has expanded 300-fold over the past two decades⁹, and this immense growth necessitates the development of next-generation NVM technologies that provide significant storage capacity and high-speed performance. Current computer architectures face three well-known barriers: memory, instruction level parallelism (ILP), and power¹⁰. Although complementary metal-oxide semiconductor (CMOS) technology represents a tractable alternative for these issues, it encounters obstacles such as reliability, leakage, and cost, which have slowed traditional device scaling. To sustain computing advancements, alternative architectures and technologies (including quantum, molecular, and neuromorphic computing) alongside emerging devices (such as memristors, quantum dots, and spin-wave devices) must be explored. Intelligent computing systems imitate the signal processing, learning, and memory functions of the human brain. This is in contrast to conventional computers built on the von Neumann architecture, in which the storage and processing of data take place in distinct units. Intelligent computing approaches enable highly efficient real-time processing of large datasets. Moreover, with their compatibility, zero standby power, scalability, and high density, memristors offer promising solutions for new computing paradigms¹¹. Recently, the development of in-memory computing has gained momentum due to advancements in memristor-based technologies, such as resistive memories, phase-change memory (PCM), magnetic random-access memory (MRAM), and ferroelectric random-access memory (FeRAM)^{12,13}. Oxide and phase-change memories are leading candidates for integration into commercial platforms due to their compatibility with the CMOS process. In addition, researchers are investigating memristive

¹School of Electrical Engineering, Korea University, Seongbuk-gu Seoul, Republic of Korea. ²Computational Electronics and Nanoscience Research Laboratory, School of Nanoscience and Biotechnology, Shivaji University, Kolhapur, India. ³Department of Physics and Nanotechnology, SRM Institute of Science & Technology, Kattankulathur, Tamil Nadu, India. ⁴Functional Materials and Materials Chemistry Laboratory, Department of Physiology, Saveetha Dental College & Hospitals, Saveetha Institute of Medical & Technical Sciences, Saveetha University, Chennai, Tamil Nadu, India. ⁵These authors contributed equally: Kiran A. Nirmal, Dhananjay D. Kumbhar. ✉e-mail: tdd.snst@unishivaji.ac.in; tgkim1@korea.ac.kr

effects in various materials to improve critical metrics, such as switching energy, speed, endurance, and retention, while also aiming for cost reductions^{12,14–17}. A memristor with reconfigurable history-dependent resistive switching can emulate the synaptic functions of biological synapses, making it one of the most promising technologies for building analog neural networks in neuromorphic computing applications^{18–21}.

The rapid advancement in digital technologies has prompted a significant transformation in the field of memory applications, marked by various innovations, expanded uses, and notable economic and environmental impacts. Developments in the field of memory technologies, including NAND flash, 3D XPoint, and emerging non-volatile memories such as MRAM and resistive random-access memory (ReRAM), are driving this revolution. These innovations offer substantial improvements over traditional DRAM and HDD storage solutions in terms of speed, density, and durability²². The effects of these advances are far-reaching, enabling faster data processing and retrieval in consumer electronics, empowering high-speed computing in data centers, and facilitating advancements in AI and ML. Additionally, integrating high-performance memory with edge devices is accelerating the development of the Internet of Things (IoT), enabling real-time data analysis and systems that are smarter and more responsive²³.

Memristors composed of two-dimensional (2D) materials have recently gained significant research interest due to their promising properties (Fig. 1)²⁴. These materials bring significant advantages to memristor technology, including low switching voltages and decreased power consumption due to their ultra-thin foot-print^{25–27}. Unlike ultrathin oxides, these materials do not have dangling bonds, which helps in avoiding scalability issues²⁸. Moreover, the thinness of the 2D semiconductor channel allows for precise gate voltage control and could mitigate short-channel effects, paving the way for multiterminal mem-transistor development^{29–31}. Additionally, the ability to stack various 2D materials in van der Waals heterostructures (HSs) circumvents challenges related to lattice matching and processing constraints^{32,33}. These materials also possess a high surface-to-volume ratio, enhancing their sensing capabilities^{34–36}, while their flexibility, rapid response times, and broad operational temperature ranges make them ideal for advanced device applications (Fig. 1)^{25,29,37,38}.

Dynamic and promising candidate

Memristors with nonlinear and non-volatile resistive switching are renowned for their small size, quick operation, and low power consumption, rendering them potential components in the expanding NVM industry³⁹. Further advantages of memristors over traditional memory devices include faster read/write speeds, stable non-volatile states, a high level of integration, and larger storage densities. In addition, memristors can be programmed and reconfigured, allowing them to adapt to various storage requirements for different applications. When a voltage is applied, memristors modulate the resistance of the functional layer to store information. Notably, memristors can record both the past resistance state and changes in charge flow, simulating the plastic response of synapses to signal stimulation, which is a process that is strikingly similar to the brain's computational processes. Memristors with multiple analog states can also store and process information, which is known as in-memory computing. Employing memristors for in-memory or near-memory computing offers a highly parallel strategy to overcome the “memory wall” challenge, which is a core limitation of the traditional von Neumann architecture⁴⁰. This traditional architecture separates data processing and storage, resulting in low efficiency for data-intensive operations due to the significant time and energy required to transmit data between the memory and processing units^{41,42}. Device endurance, switching energy, switching time, state retention time, device size, and operating voltage are the most prominent advantages of memristors for commercial applications¹⁹. Memristors can replicate specific roles of biological neurons and synapses, including synapse-like plasticity and neuron-like integration and spiking. In addition, the resistance/conductance of memristors acts as a proxy for synaptic strengths, which can be adjusted using local learning rules. One widely applied rule is spike-timing-

dependent plasticity (STDP), where conductance or another local state variable is adjusted dynamically based on spike timing. This method embodies the principle of “computing with time, not just in time”⁴³. Many materials have been investigated to study their memristive characteristics, including low-dimensional materials^{44,45}, perovskites^{46–48}, polymers⁴⁹, organic materials^{50,51}, 2D materials^{52–54}, transition metal oxides (TMO)^{55–57}, and structured inorganic materials^{58–61}. The widespread availability of binary oxides, coupled with their adaptable fabrication using diverse techniques (such as sol-gel processes, atomic layer deposition, magnetron sputtering, physical and chemical vapor deposition, pulsed laser deposition, and hydrothermal methods) underpins their significant role in memristor research, particularly those involving TMO⁶². Moreover, various metal oxides have been explored extensively, including TiO₂⁵⁵, CuO₂⁶³, HfO₂⁶⁴, TaO_x⁶⁵, and Y₂O₃⁶⁶. Unlike transistor-based technology, which uses many devices to replicate biomimetic functions, memristors inherently embody simple biomimetic functions. However, despite the rapid increase in memristor research, further advancements are required in terms of power efficiency, reliability, multifunctionality, tunability, and hetero integration. Thus, the post-Moore computing era will center on developing smart devices and materials and creating new architectures to use them effectively.

2D materials and their properties

2D materials are atomically thin layered materials with either a single layer or a few layers of atoms and thicknesses typically less than 1 nm. The unique and hallmark feature of these materials is the bonding interactions in the stack. While weak van der Waals interactions occur across layers, atoms in the layer are ligatured by saturated covalent bonds⁶⁷. The discovery of exfoliated monolayers (or few-layer graphene) and their exceptional properties has also sparked significant interest in 2D materials^{5,68}. Inspired by graphene, researchers have explored various classes of other ultrathin 2D nanomaterials, such as transition metal dichalcogenide (TMDC), metal oxides, hexagonal boron nitride (h-BN), metal carbides or nitrides (MXenes), layered double hydroxides (LDHs), and a family of mono elemental compounds (including black phosphorus, 2D perovskite, arsenene, antimonene, and bismuthine)^{69,70}. These materials are highly compatible with conventional CMOS technology, allowing straightforward synthesis and integration onto diverse substrates and facilitating a broad array of applications. Each 2D material exhibits distinct electrical and optical properties, which are influenced by its chemical composition, crystal structure, and thickness. For example, graphene is known for its excellent conductivity, making it a favored electrode choice in memristive devices⁷¹. TMDCs, such as MoS₂ and WSe₂, exhibit semiconducting behavior, which is essential for modulating resistive states in memory and neuromorphic applications⁷². The layer-dependent bandgap of WSe₂ allows for unique ambipolar transport properties, while monolayer TMDCs exhibit strong light-matter interactions, making them ideal for optoelectronic applications. Additionally, the unique ambipolar characteristics and low doping levels of 2D WSe₂ enable strong spin/valley coupling, enhancing its potential for valleytronic and spintronic applications⁷³. Among TMDCs, Group V compounds (such as V, Nb, and Ta) exhibit metallic behavior, while Group VI compounds (including Mo and W) can display either semiconducting or metallic properties based on their crystal structure. Monolayer TMDs are particularly noteworthy for their high exciton binding energies and valley polarization, which position them as key components in vertical van der Waals heterostructure devices⁷⁴. Materials such as PtSe₂ exhibit tunable bandgaps, which makes them suitable for broadband photodetectors. Black phosphorus (or phosphorene) is notable for its high carrier mobility and direct band structure⁷⁵.

Emerging materials, such as MoTe₂, offer direction-dependent properties, ultrahigh carrier mobility, and broad-spectrum light absorption, enhancing their utility in advanced memory and optoelectronic devices⁷⁶. Hexagonal h-BN stands out as an effective dielectric material in memristors, supporting bipolar resistive switching and non-volatile storage due to its wide bandgap and chemical stability. However, the potential of h-BN-based memristors in low-power digital logic and neuromorphic computing

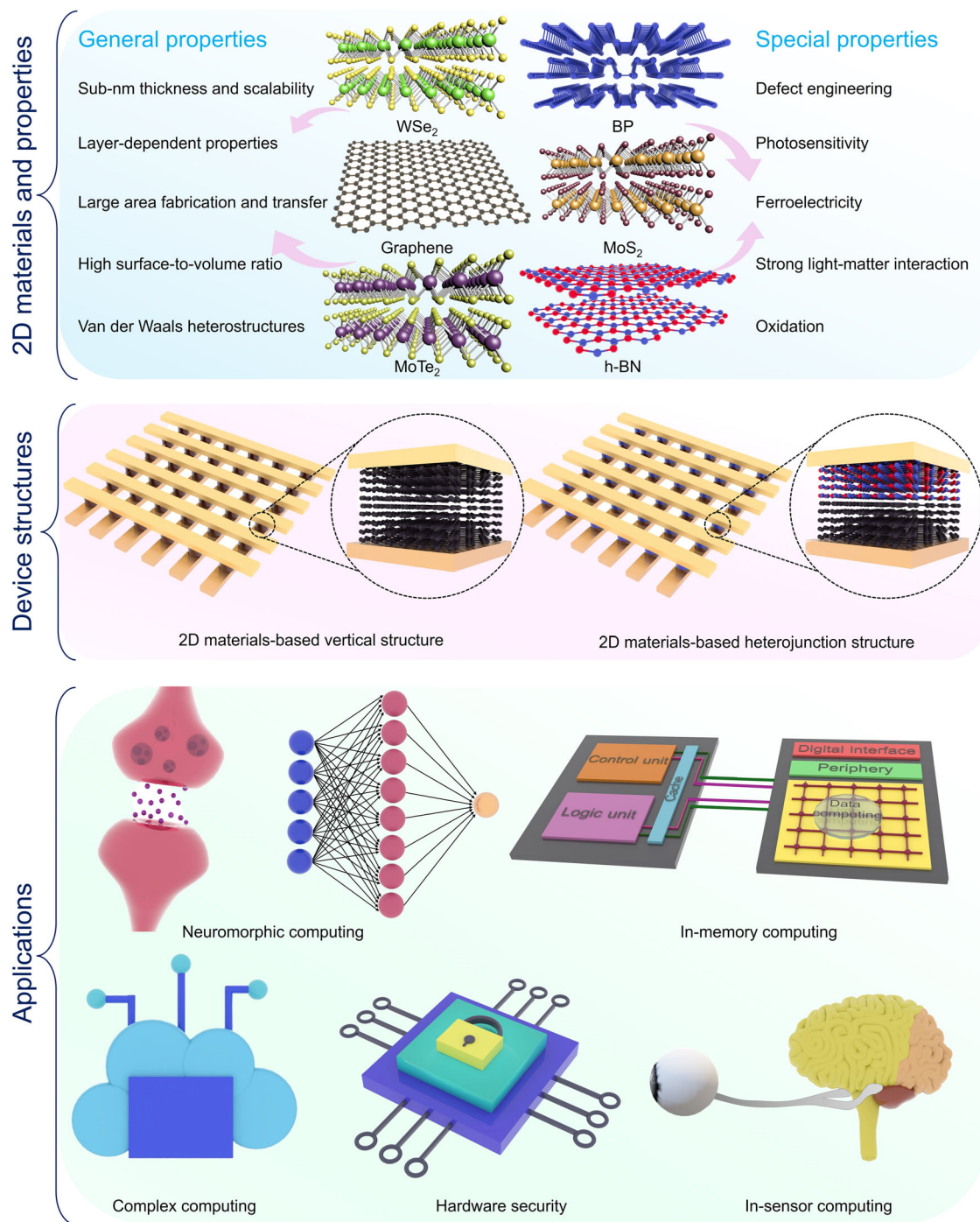


Fig. 1 | Schematic illustration of different 2D materials and devices. Some illustrative examples of 2D materials and their properties. Types of memristive devices based on layered 2D materials (i.e., vertical memristor and heterojunction

memristor). Applications of 2D memristors in neuromorphic computing, in-memory computing, complex computing, hardware security, and in-sensor computing. Adapted from ref. 68.

remains largely unexplored. Continued research into these diverse 2D materials could unlock innovative applications in low-power devices and neuromorphic systems, significantly enhancing performance and energy efficiency in next-generation technologies⁷⁷.

Due to their atomic-level thickness, 2D materials offer substantial reductions in energy consumption by mitigating short-channel effects, optimizing efficiency, and enabling further device miniaturization, similar to the integration levels of neurons and synapses in the human brain. Additionally, 2D materials feature pristine surfaces that are devoid of any dangling bonds and exhibit distinctive physical properties. This approach presents a crucial pathway to sustain Moore’s law, leveraging the previously

mentioned notable qualities of 2D materials to advance the fabrication of solid-state electronic devices⁷⁸. The progress in advanced 2D materials (such as MoS₂⁷⁹, HfSe₂⁸⁰, h-BN⁸¹, and MXenes⁸²) has made it feasible to create vertically structured memristors with cross-bar arrays that possess a higher density. Recent advancements in 2D material-based memristors have also exhibited significant progress. These new memristors demonstrate remarkable performance characteristics, such as an on/off ratio reaching up to 10¹¹, low SET voltages (as low as 0.05 V), outstanding retention and endurance of up to 10⁵ s and 10⁷ cycles, respectively, fast switching speeds of 1.5 ns, and exceptionally low power and energy consumption (measured at 1 fW and 8.8 zJ, respectively)⁸³.

The unique properties of the various 2D materials, coupled with different switching mechanisms, offer distinct advantages for memristive devices. High on/off ratios and low operating voltages enhance device performance and energy efficiency, while flexibility and mechanical strength enable the development of flexible and wearable electronics. Additionally, tunable electronic properties and compatibility with other materials allow for the design of multifunctional devices tailored to specific applications. Table 1 provides a concise overview of the properties, features, and potential applications of various 2D materials and their memristor implementations.

Operational mechanisms of 2D materials-based memristors

Although memristive and neuromorphic devices may exhibit structural similarities, the carrier transport mechanisms that govern their fundamental operating principles can differ depending on their atomic composition. In the following section, we discuss five widely recognized mechanisms responsible for memristive and neuromorphic behaviors: redox reactions, vacancy migration, phase transitions, Schottky emissions, direct tunneling, and charge trapping/de-trapping, as illustrated in Fig. 2.

Redox reaction

Conductive filament formation is a fundamental mechanism in resistive switching memory devices. By adjusting the input voltage pulse or bias sweep, memristive behavior and artificial synaptic functions can be mimicked through the creation and regulation of these filaments, as depicted in Fig. 2a. This was demonstrated by Zhao et al.⁸⁴ in an Ag/MoTe₂/ITO device, where resistive switching is driven by the formation of conductive filaments from Ag ions, which migrate from the Ag top electrode (TE) under an applied bias. When a reverse bias is applied, the filament dissolves, returning the device to a high-resistance state (HRS). This volatile switching behavior aligns with the essential characteristics of artificial neurons. Moreover, this mechanism is particularly effective in 2D materials (such as MoS₂⁸⁵, WS₂⁸⁶, MXene⁸⁷, ZrO₂⁸⁶), in which filaments can be reliably formed and disrupted, enabling efficient switching between high and low-resistance states. The atomic thickness of these materials allows for precise control over filament formation, which is critical for enhancing device scalability and performance.

Vacancy migration

Vacancy migration involves the movement of vacancies within the material, which can alter local conductivity. As these vacancies shift, they create paths for charge carriers, affecting the resistive switching mechanism, as shown in Fig. 2b. Khot et al.⁵² demonstrated this mechanism in a Pt/Ti₃C₂/Pt memristor, where oxygen vacancies play a key role in the formation and dissolution of the conductive filament. The filament starts forming at the bottom electrode (BE) due to the drift of oxygen vacancies when a positive voltage is applied to the TE. As the voltage increases, the filament grows fully, reducing the resistance and switching the device from an HRS to a low-resistance state (LRS). When the voltage is reversed, oxygen vacancies migrate back toward the TE, causing filament rupture and restoring the device to the HRS. This mechanism is significant in 2D materials such as black phosphorus and TMDCs, where vacancies can be introduced and controlled to modulate the electrical properties of the device^{29,88}. The high mobility of vacancies in 2D materials enhances the speed and efficiency of the switching process.

Phase transition

TMDCs in their 2D form are composed of ultrathin layers and exhibit stable phases that define their properties⁸⁹. Extensive research has focused on controlling these phase transitions, highlighting their suitability for memristive and neuromorphic computing⁹⁰. The switching mechanism based on phase transition is portrayed in Fig. 2c. Hou et al.⁹¹ reported a phase change memristor using strain engineering to induce a strain-driven semi-metallic-to-semiconducting phase transition in MoTe₂. By tuning the material close to its phase transition boundary, these devices demonstrate impressive performance, including low switching voltages of 90 mV, on/off ratios of 10⁸, switching times of 5 ns, and retention times exceeding 10⁵ s.

Schottky emission and direct tunneling

Schottky emission and direct tunneling mechanisms play a critical role in understanding the switching dynamics of 2D memristors (Fig. 2d). These mechanisms enable low-power operation and rapid switching, making them suitable for next-generation memory and neuromorphic computing applications. In a study conducted in 2023, Lei et al.⁹² investigated the impact of material thickness on both volatile and non-volatile switching behaviors through Schottky barrier height modulation. Their findings revealed that devices with fewer layers struggle to maintain their LRS because electrons can escape the conduction band and occupy trap sites when no bias voltage is applied. This escaping of electrons results in an increased Schottky barrier height over time, causing the device to transition back to its HRS. Interestingly, adding more material layers extends the duration of this process, enhancing the resistive states. These insights are significant for developing devices capable of sustaining their states for specific periods, which can be leveraged to create synaptic elements for neuromorphic applications.

Charge trapping

The charge trapping mechanism in 2D memristors is a vital component that influences their performance and potential use in advanced memory and neuromorphic devices (Fig. 2e). Seo et al.⁹³ developed optical-neural synaptic devices by integrating synaptic and optical sensing functions within an h-BN/WSe₂ heterostructure. The operation of this van der Waals (vdW) synaptic device relies on the trapping and detraping of electrons. It functions with low voltage spikes of just 0.3 V and consumes only 66 fJ per spike.

Memristor beyond conventional memory applications

In the post-Moore era, the focus is on developing systems that emulate AI, leveraging innovations such as in-memory computing and non-von Neumann architectures. These systems are tailored to execute cognitive tasks, including object recognition, association, adaptation, and learning, prioritizing high energy efficiency and parallelism. Memristor devices are distinguished by their ability to overcome the von Neumann bottleneck at the nanoscale level, seamlessly integrating memory and computation. One innovative approach leveraging this capability is “in-memory computing,” which uses memory to perform computations directly at the data storage site. Various studies have examined using memristors across diverse domains, including storage⁴⁹, hardware security⁹⁴, neuromorphic computing⁶², in-memory computing⁶⁸, in-sensor computing⁹⁵, and high-frequency RF applications⁹⁶. As memory applications continue to evolve, they promise to catalyze the next wave of technological breakthroughs and propel progress across a spectrum of industries, from healthcare to autonomous vehicles, and beyond.

This review focuses on memristors based on layered 2D materials and their applications beyond memory. We begin with a brief introduction to the memristor timeline and its general applicability. Next, we discuss the use of memristors in neuromorphic computing, followed by an exploration of the realistic potential of memristors for diverse applications. Finally, we outline both the opportunities and challenges confronting current memristor systems that use 2D layered materials, while envisioning a bright future for the hardware realization of brain-like neural architectures.

Neuromorphic computing

Understanding synaptic plasticity

Neuromorphic computing is inspired by biological neural networks and has generated significant attention as a novel paradigm for data processing, storage, and advanced tasks, such as cognition, inference, and learning⁹⁷. Memristors are crucial for replicating the functions of the human brain, which has approximately 10¹¹ neurons and 10¹⁵ synapses and is an incredibly effective and flawless information-processing device⁹⁸. To understand the significance of memristors in neuromorphic systems, it is essential to examine the concept of synapses, which are categorized as excitatory or inhibitory based on the type of neurotransmitter receptors present on the synaptic membrane. In neuroscience, synaptic plasticity refers to the strength of the connections (or synapses) between nerve cells⁹⁹.

Table 1 | Overview of the properties, features, and potential applications of various 2D materials and their memristor implementations

Materials	Material properties	Memristor features	Applications	Ref.
MoS ₂	moderate bandgap, high stability	low programming voltages	memristor-based neural networks, bio-realistic synaptic emulation, photodetector, in-sensor computing	184
MoSe ₂	high electrical conductivity	more reliable and faster operation	neuromorphic computing, nociceptive emulators, in-sensor computing	185
WS ₂	tunable bandgap, unique semiconductor properties	longer retention time, low operating voltage, mechanical robustness	flexible memristor, photodetector, in-sensor computing	72
WSe ₂	ambipolar transport properties, strong spin/valley coupling	good stability, reliability, excellent reproducibility	synaptic emulation, photodetector, in-sensor computing	73
NbSe ₂	superconductivity at low temperatures, mechanically robust	improved memory characteristics, DC switching	neurological system, analog signal processing, quantum computing	186
BP	natural direct band gap, broad light absorption range, high carrier mobility	forming free operation, low operational voltage, high memory window	transparent and wearable electronic, optoelectronics, energy storage, AI	75
MXene	high metallic conductivity, excellent mechanical properties, super hydrophilicity	functional layer, electrode, excellent memory window, good memory retention	intelligent devices, radio frequency devices, energy storage, neuromorphic computing	50,52
Graphene	low manufacturing cost, high mechanical flexibility, high optical transparency, high electrical conductivity	functional layer, electrode material, high speed, low power operation	optical memristors, photo-synapse, flexible electronic sensors	70
BN	wide bandgap, mechanical and environmental stability, excellent transparency	multi-state analog programmability, low-power consumption digital logic function	printing electronics, ultrathin flexible memory, radio-frequency switches, neuromorphic computing	54,77
VSe ₂	unique and outstanding electronic and spintronic properties	decent and reliable TS behaviors	logic operations of "NOT", "AND" and "OR", ANN	187
MoTe ₂	polymorphism, ultrahigh carrier mobility	Low power	synaptic plasticity, arithmetic functions	76
ZrO ₂	high thermal stability, phase transformation, scalability, high mechanical strength	lower V _s and V _R threshold voltages, faster switching speed, longer retention	artificial synapses, ANN, flexible electronics, sensor technology, analog computing	86
SnS	p-type conductivity, controllable carrier density, cost-effective, environmentally friendly, tunable bandgap	low power, ultrafast, emulated wide range of synaptic plasticity behaviors	artificial synapse, photodetector, in-sensor computing	60
SnSe	p-type conductivity, more energetically favorable for the migration of metal ions	low operation voltage, fast switching speed, and a high on/off ratio	future multifunctional neuromorphic devices	188
GaSe	p-type semiconductor, excellent optical and electrical properties	long-term performance	optoelectronics, resistive switching, multi-functional device	189
Sb ₂ S ₃	high surface area, tunable bandgap, excellent electronic characteristics	low operational voltages, robust endurance, reliable switching behavior	optoelectronics, resistive switching	152

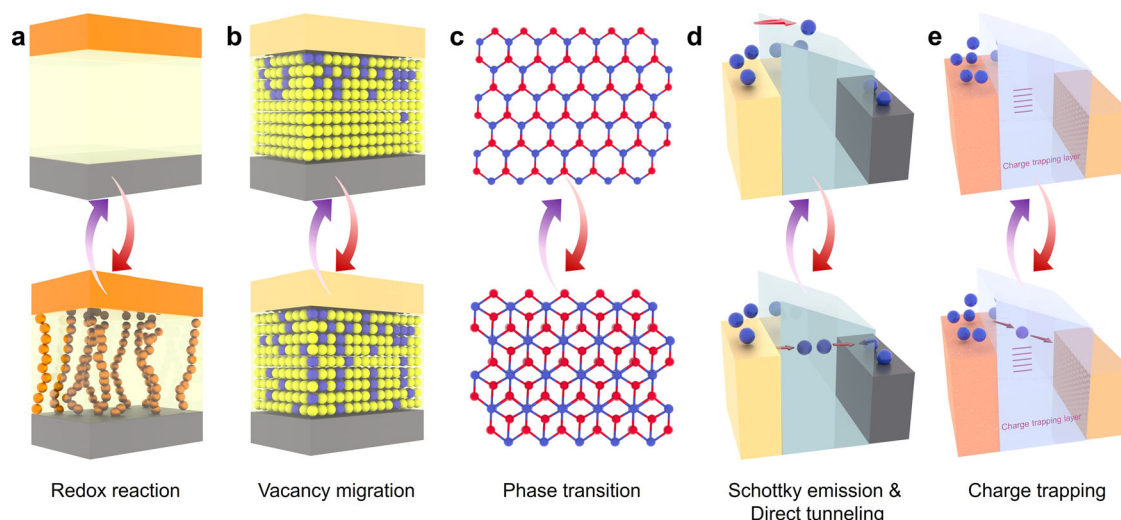


Fig. 2 | Representative operational mechanisms of memristor devices based on 2D materials. Conductive filament formation by **a** redox reaction and **b** vacancy migration, **c** phase transition, **d** Schottky emission and direct tunneling, and **e** charge trapping. Adapted from ref. 181.

Synaptic plasticity executes the following functions: long-term plasticity (LTP), which is responsible for memory and learning, and short-term plasticity (STP), which is associated with cognitive functions involving spatiotemporal information⁵. Synaptic devices are used for STP in various fields, including sensory processing, spatiotemporal pattern processing, speech recognition, and adaptive learning¹⁰⁰. Paired pulse facilitation (PPF) is a type of STP that usually involves the amplification of signals in sequentially evoked post-synaptic potentials. The term paired-pulse depression (PPD) describes a reduction in the intensity of synaptic transmission following an action potential burst or high-frequency stimulation. This reduction helps prevent overstimulation and maintains balance within neural circuits. In neuromorphic systems, PPD is crucial for regulating synaptic activity and ensuring stable performance. A comprehensive overview of neuromorphic computing is summarized in Table 2.

By incorporating PPF and PPD, neuromorphic computing systems can achieve more realistic and adaptive signal processing that closely emulates the dynamic behavior of biological neural networks. Other forms of plasticity include STDP, spike-rate-dependent plasticity (SRDP), and spike-amplitude-dependent plasticity (SADP). Typically, STP and LTP determine the fundamental characteristics of distinct biological synapses. However, understanding how neurons communicate via STDP and SRDP pathways requires insight into the connections between multiple synapses. The fundamental concept of synaptic plasticity, as elucidated by Donald Olding Hebb, is popularly known as Hebbian theory. This theory proposes that consistent and repetitive stimulation to presynaptic neurons can improve synaptic transmission efficiency⁹⁹. The notion of “cells that fire together, wire together” is frequently used to summarize this concept. Asymmetric STDP reveals Hebbian learning, while symmetric STDP reveals anti-Hebbian learning. Furthermore, SRDP refers to changes in synaptic strength based on the rate or frequency of spikes rather than their precise timing. In contrast, SADP involves changes in synaptic strength based on the amplitude of spikes or the strength of the post-synaptic response¹⁰¹.

Recent innovations

Recent advances have showcased promising developments in memristors. For instance, Yan et al. successfully developed a memristor based on 2D WS₂ nanosheets with a low switching speed and effective synaptic functionalities (Fig. 3a)¹⁰². The device operated at low SET and RESET voltages of +0.6 and -0.2 V, respectively (Fig. 3b). Moreover, the device displayed PPF behavior, as presented in Fig. 3c, with the applied pulse for the measurement illustrated in the inset of Fig. 3c. The memristor effectively simulated learning and memory processes under STDP, as well as the transition from STP to

LTP. It also exhibited excitation and inhibition responses to positive and negative pulse-stimulus trains. Similarly, Meng et al. introduced a flexible, low-dimensional memristor using BN that could effectively mimic four basic STDP rules⁷⁷. Khot et al. explored a novel memristive device fabricated from amorphous BN (a-BN)⁵⁴, highlighting its stability, endurance, power consumption, and efficiency for high-density memory storage. Figure 3d illustrates a vertical configuration of a memristor cell, where Ag functions as the TE, a-BN operates as the switching layer, and Pt is used for the bottom electrode. The SET operation occurs at +0.4 V, while the RESET operation is observed at -1.5 V. By applying precisely timed pulses to the pre- and post-synaptic terminals, the authors effectively recreated classical Hebbian STDP rules. For example, the a-BN-based electronic synapse accurately replicated symmetric Hebbian (Fig. 3e), symmetric anti-Hebbian, anti-symmetric Hebbian, and anti-symmetric anti-Hebbian (Fig. 3f) STDP rules. The observed potentiation and depression behaviors differed based on the timing of the pre-synaptic and post-synaptic spike inputs to the electronic synapse, demonstrating the variations across the four STDP rule types. In addition, a neural network built on these rules achieved 90.8% pattern accuracy. Their study reveals that 2D material-based memristors can effectively emulate synaptic functions, which are crucial for future applications in advanced computing systems and enable more efficient data processing and storage.

In another significant advancement, the Thean group achieved integration of wafer-scale 2D MoS₂ memristor arrays using a solution processing method¹⁰³. A schematic of the Ti/Pt-MoS₂-Ti/Pt device is displayed in Fig. 3g. Due to its linear conductance update characteristics, this MoS₂ memristor achieved a high analog on/off ratio, extended memory retention, low device fluctuations, and outstanding endurance. The device's operation is driven by thermionic and tunneling transport mechanisms. Moreover, MoS₂ memristors can demonstrate analog potentiation and depression across various resistive states (Fig. 3h), with an impressive on/off ratio of 160. Memristors with a high analog on/off ratio are beneficial for neural networks that require access to various synaptic weight values. Additionally, the MoS₂ memristor demonstrates good linear weight/conductance update properties, which is useful for high-performance neuromorphic computing applications (Fig. 3i).

Abrupt heterojunctions with perfect band alignments can be precisely engineered because the surfaces of 2D materials are free of dangling bonds and trap states⁹⁷. Researchers have engineered precise heterojunctions using 2D materials. For example, Khot et al. reported a filament formation-mediated heterojunction memristor using GeTe/MoTe₂ as an active switching layer (Fig. 3j)¹⁰⁴. The device exhibited switching behavior at very

Table 2 | Comparative characteristics of memristor devices based on 2D materials for neuromorphic computing

Device structure	Working principle	Thickness (nm)	Device area (μm^2)	Switching voltage (V)	Energy consumption	Power consumption	Synaptic function	Ref.
Pd/WSe ₂ /Pt	Trap assisted tunneling	200	-	+0.6, -0.2	299.8 fJ	13	PPF, STDP	102
Al/Ti ₃ C ₂ /Pt	Ion/vacancy migration	300	-	± 3	-	-	STDP	52
Ag/Ti ₃ C ₂ T _x /Pt	Ion/vacancy migration	200	-	+1.33, -0.94	-	230 nJ	STDP, PPF, PPD, CNN	53
Ag/SnS/Pt	Ion/vacancy migration	10–40	-	± 0.2	-	100 fJ	STDP, DNN	115
Ag/Ag-GeTe/Ag	Ion/vacancy migration	60	25	+0.18, -0.2	-	-	STDP	190
Ag/MoTe ₂ /ITO	Ion migration	1.5 μm	200	+1, -1.5	74.2 pJ	-	STDP, PPF, PTP	84
Ta ₂ N/BN/ITO	defects-based CF	-	-	+0.7, -0.6	-	-	EPSC, IPSC, PPF, STDP	77
Ti/Pt-MoS ₂ -Ti/Pt	Tunneling	2.6	25	+0.65, -0.90	-	-	P&D, GPU	103
Cu/MoS ₂ /Au	Ion migration	-	4	+0.25, -0.15	-	-	STDP	126
Cu/MoTe ₂ /Si	Ion migration	-	200	+1.9, -2.16	-	-	STDP, PPF, EPSC	76
Au/ReSe ₂ /Au	Ion/vacancy migration	1	4	+3, -0.5	-	-	LTP, LTD, MNIST	191
Ag/WSe ₂ QDs/ La _{0.3} ST _{0.7} MnO ₃ /SrTiO	-	97	90	+0.52, -0.19	-	0.16 nW	STDP, EPSC, PPF, MNIST	192
Gr/ (PEA) ₂ PbBr ₄	Hopping and DT	40	1–35	+2.8, -1	400fJ	-	PSC	193
Ag/GeTe/MoTe ₂ /Pt	Ion/vacancy migration	20	5–15	+0.15, -0.14	30nJ	-	STDP, EPSC, PPF, MNIST	104
Au/Ti/MoTe ₂ /MoS _{2-x} O _x /SiO ₂ /Si	Ion migration	-	-	± 5	-	-	STDP, PPF CNN,	194
Ag/SnS/Pt	Ion/vacancy migration	300	-	+0.22 -0.20	-	-	STDP, EPSC, IPSC, PPF, PPD	60
Ag/MoO _x /MoS ₂ /Ag	Vacancy migration	20–30	-	± 0.2	-	10 nW	STM, LTM	195
Ag/WO _{3-x} /WSe ₂ /Gr	Vacancy migration	10	-	± 0.2	-	0.1 nW	LTM, STM, PPF, hetero-synaptic behavior	196
Pt/MoSe ₂ /Pt	Vacancy migration	1.9	-	± 5	-	-	STP, PPF, LTP, LTD	185
Ag/WSe ₂ /Ag	Ion/vacancy migration	3.4	-	± 4	-	-	P&D, PPF, STP, LTP	73
Ag/NbSe ₂ /HfO ₂ /Pt	Ion/vacancy migration	2/12	100	+0.73, -0.3	-	-	PPF, PTP, EPSC	186
Pt/WSe ₂ /Pt	Vacancy migration	-	-	+1.4, -0.44	-	-	LIF, ANN	187
Ag/ZrO ₂ /WS ₂ /Pt	Ion migration	35/65	-	+7.5, -5	-	-	STDP, PPF, MNIST	86
Cr/Au/SnSe/Ag	Ion/vacancy migration	21.7	25	0.6	-	-	artificial nociceptor, SNN	188

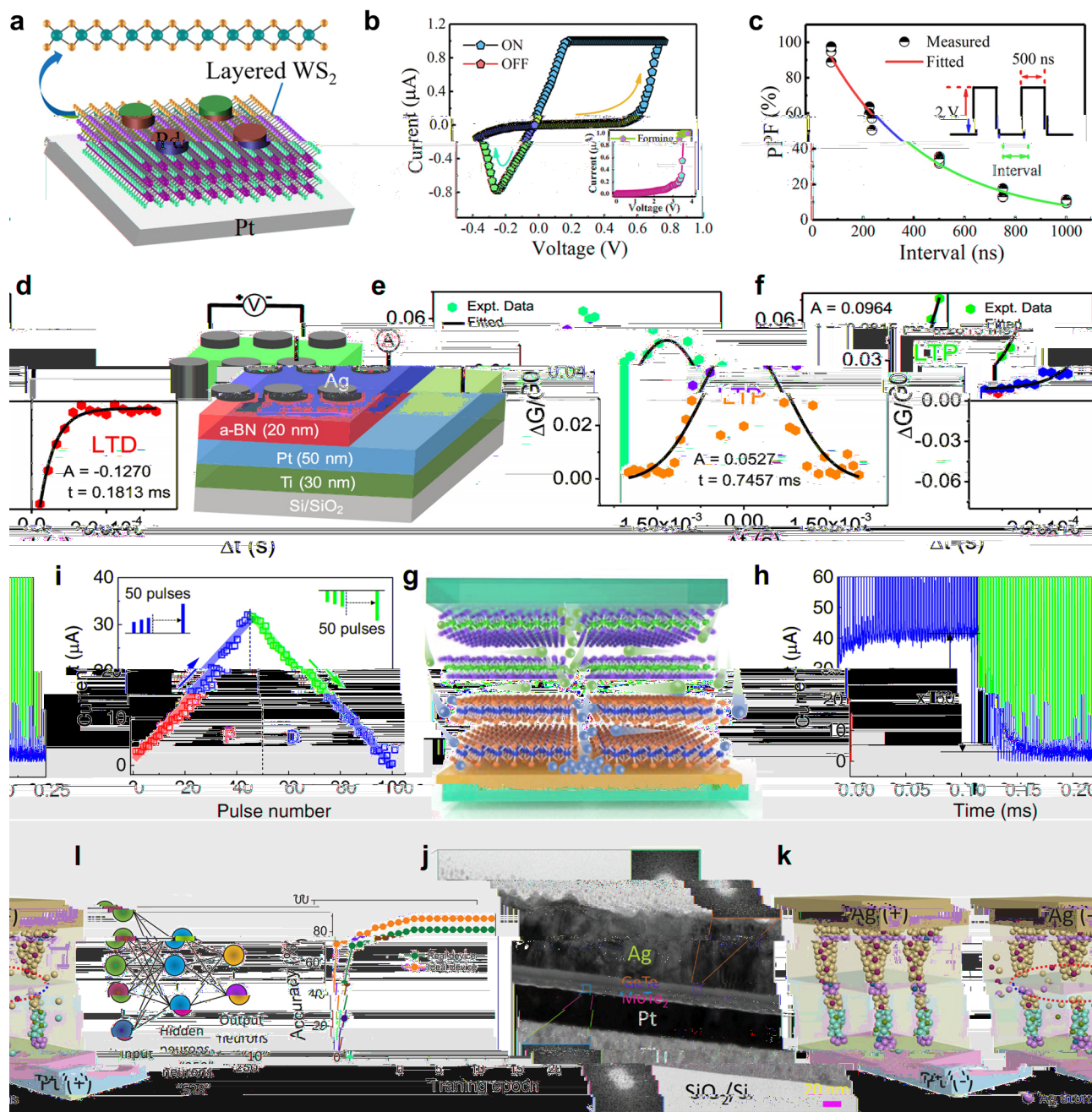


Fig. 3 | 2D memristors for neuromorphic computing. **a** Schematic of Pd/WS₂/Pt memristor. **b** Typical I-V characteristics of the device. **c** PPF index change with the time interval between a pair of pulses. Reprinted under terms of the Creative Commons license from ref. 102. © Wiley-VCH GmbH, Weinheim. **d** Schematic representation of Ag/a-BN/Pt memristor. Mimicking **e** symmetric Hebbian and **f** anti-symmetric anti-Hebbian STDP rules. Reprinted under terms of the Creative Commons license from ref. 54. Copyright © 2022, American Chemical Society **g** Device structure of Pt/MoS₂/Ti memristor along with its **h** potentiation and depression characteristics. **i** Conductance update as a function of incremental

potentiation and depression pulse numbers. Reprinted under terms of the Creative Commons license from ref. 103. Copyright © 2022. **j** Cross-sectional high-resolution TEM image of the GeTe/MoTe₂ heterostructure memristor with their respective FFT images showing heterointerfaces. Schematic illustrating the RS mechanism during **k** ON condition (filament formation through Te vacancies and Ag oxidation reaction) and OFF condition (rupturing the conductive filament). **l** Schematic of multilayer perceptron and pattern recognition accuracy of GeTe/MoTe₂ heterostructure memristor. Reprinted under terms of the Creative Commons license from ref. 104. © Wiley-VCH GmbH, Weinheim.

low switching voltages ($V_{SET} = +0.15$ V and $V_{RESET} = -0.14$ V) with minimal energy consumption (≈ 30 nJ), a high memory window, long retention time (10^4 s), and excellent endurance (10^7 cycles). The exceptional switching ability of the Ag/GeTe/MoTe₂/Pt HS device was attributed to the controlled formation and growth of the Ag conductive filaments, with Te vacancies assisting filament formation (Fig. 3k). The localized formation and expansion of filaments within the hetero bilayer enhance the reliability and stability of the resistive switching characteristics by minimizing variabilities in

the nucleation and breakdown of the conduction filaments. Furthermore, the authors mimicked various STDP rules. Finally, the practicality of the GeTe/MoTe₂ memristor was investigated by implementing a multilayer perceptron for pattern recognition applications. To achieve this, they used a multilayer perceptron with 528 inputs, 250 hidden neurons, and 10 output neurons (Fig. 3l). The fabricated device exhibited a linear conductance change, significantly improving the recognition accuracy to 81.3% (Fig. 3l). Based on these findings, 2D HSS are expected to improve switching voltage,

endurance, retention, and synaptic learning properties compared to single layer memristors.

Neural networks

Currently, there are two types of neural networks popular among researchers: artificial neural networks (ANNs), which use backpropagation and linkage relations, and spiking neural networks (SNNs), which use neuron models and spike signal transfer. ANN algorithms have demonstrated exceptional efficacy and have significantly advanced the field, evolving into more sophisticated forms such as deep neural networks (DNNs) and convolutional neural networks (CNNs)^{62,105}. ANNs are composed of interconnected neurons that manage input voltage signals, process them through a crossbar array, and produce the output as electric currents. This processing includes linear transformations through multiply-accumulate (MAC) operations, complemented by nonlinear adjustments performed by the neurons^{80,106,107}. The crossbar array represents the network's interconnected nodes. In many current implementations, classification is accomplished offline, with the trained weights being stored in memristive devices within the array^{80,107,108}. In contrast, SNNs use neuron models and spike signal transfer to closely mimic biological neural processing. They encode information using sparse and asynchronous binary spikes, allowing for a more faithful emulation of human brain functions on artificial neuromorphic hardware. This design enhances noise resilience and energy efficiency while facilitating spatiotemporal learning mechanisms, such as STDP¹⁰⁹. The distinct computational approaches of ANNs and SNNs significantly influence their applications, particularly in the choice of neuron configurations and design principles.

A variety of neuron models have been proposed to emulate biological neurons, including the McCulloch-Pitts (MP) model¹⁰⁹, the Hodgkin-Huxley (H-H) model¹¹⁰, the integrate-and-fire (IF) model¹¹¹, and the leaky integrate-and-fire (LIF) model¹⁰⁹. Each model offers unique features for simulating neuronal behavior, contributing to our understanding of neural dynamics and informing the development of artificial systems. Among these, the LIF model is particularly important in constructing SNNs. LIF neurons replicate biological behavior by integrating incoming signals until a specific threshold is reached, at which point they release a spike. This model includes a leaky term that allows the membrane potential to gradually decay over time, introducing vital temporal dynamics. LIF neurons are especially suited for real-time processing of temporal information, making them ideal for applications in sensory processing and neuromorphic computing where time-dependent behavior is crucial. In contrast, bipolar switching artificial neurons operate more like traditional digital circuits, producing binary outputs based on the presence or absence of input signals. These neurons use bipolar switching characteristics to toggle between two states, facilitating faster operations and lower energy consumption¹¹². They are particularly effective in applications requiring speed and efficiency, such as conventional machine learning tasks involving large datasets and rapid inference times. However, they may not fully exploit the temporal dynamics that SNNs can offer.

The choice between LIF and bipolar switching neurons significantly influences neural network design and implementation. Applications in robotics and real-time decision-making benefit from the temporal processing capabilities of LIF neurons, while high-throughput tasks, such as image classification or natural language processing, may perform better with bipolar switching neurons due to their speed. Understanding these differences allows researchers to make decisions regarding device configurations and neuron type selection based on specific application needs. As the field evolves, exploring hybrid architectures that combine the strengths of both neuron types could result in even more advanced neural computing systems, enhancing capabilities across a wide range of applications.

Recent advancements in memristor technology have opened new avenues for neuromorphic computing, particularly in SNNs. In this context, Roldan et al. recently examined multilayer h-BN memristors in SNNs for image classification tasks¹¹³. They fabricated arrays of 5×5 μm cross-point memristors with an Au/Ti/h-BN/Au structure on 300 nm SiO₂/Si wafers.

Optical microscope images confirmed that no cracks were present, while scanning electron microscope images confirmed continuous wrinkles on both the SiO₂ substrate and the electrodes (Fig. 4a), indicating that the h-BN layers were intact. The devices exhibited clear bipolar resistive switching in response to electrical stimuli of varying polarities (Fig. 4b). Using STDP as the learning rule, they trained the SNN using the MNIST dataset, which includes 784-pixel grayscale images of handwritten digits. The network had 784 input neurons, and a corresponding excitatory layer connected to inhibitory neurons, which facilitated lateral inhibition and competition among excitatory neurons (Fig. 4c). The authors varied the number of neurons and training epochs, finding improved recognition accuracy with more neurons and saturation in accuracy for epochs beyond three (Fig. 4d, e). Additionally, Ma et al. demonstrated that an ANN chip based on MoS₂ could recognize numerals with over 97% accuracy¹¹⁴.

Lu et al. explored the development and performance of a low-power ultrafast memristor based on p-type van der Waals tin(II) sulfide (SnS) (Fig. 4f)¹¹⁵. The device exhibited outstanding performance metrics, featuring a switching voltage of approximately 0.2 V, a switching speed of under 1.5 ns, high endurance, and an exceptionally large on/off ratio of 10⁸. Each device consumed approximately 100 fJ of power during the ON state. Figure 4f depicts the ionic movements within the Ag/SnS/Pt-based crossbar structure, which is designed to mimic a biological synapse. Silver (Ag) ions from the electrode migrate into SnS, where they fill vacancies or settle in interstitial positions, migrate in response to an external electric field, and are reduced to Ag atoms at the cathode, resulting in increased density of the Ag filament. The device exhibited PPF behavior when it received a 0.65 V/50 ns pulse train with a 500 ns pulse interval, as displayed in Fig. 4g. Figure 4h illustrates 32×32 high-density crossbar arrays with a 50 nm feature size. Chip-level simulations demonstrated an on-chip learning accuracy of 87.76% for CIFAR-10 image classifications, which is close to the software accuracy of 90%. Additionally, Yao et al. demonstrated the use of memristor crossbar arrays in CNNs, achieving notable improvements in yield, performance, and uniformity¹¹⁶. By incorporating eight 2048-cell memristor arrays, they facilitated efficient parallel convolution with multiple kernels, enabling the duplication of identical kernels through shared inputs. This memristor-based CNN neuromorphic system exhibited remarkable efficiency and accuracy (>96%) in handwritten digit recognition, with scalability providing additional potential for enhancement.

Flexible memristors employing 2D materials have emerged as a promising approach in neuromorphic computing due to their exceptional electronic properties and mechanical flexibility^{77,117,118}. These devices mimic synaptic functions by offering tunable resistance states, enabling efficient information processing and storage that are similar to the human brain⁷⁷. The integration of 2D materials (such as graphene and TMDCs) in flexible memristors enhances their performance by providing high surface area, excellent electrical conductivity, and scalability^{77,117,118}. This advancement paves the way for the development of flexible wearable neuromorphic systems that are capable of sophisticated learning and adaptation, potentially revolutionizing fields such as robotics, healthcare, and AI. 2D materials have also attracted considerable research interest because of their ability to modulate the switching mechanisms¹¹⁹. These materials have been instrumental in advancing our understanding of these processes, providing insights that are crucial for the development of next-generation electronic devices^{5,106,120}. Additionally, 2D materials have been demonstrated to enhance the performance of traditional metal oxide-based memristors by improving their switching characteristics and overall reliability^{121,122}. The development of various vertical memristors that incorporate 2D materials has resulted in devices with fast switching speeds, low threshold voltages, and high electrical endurance. These characteristics make them suitable for a wide range of applications, including NVM and neuromorphic computing. Among these memristors, sandwiched devices that can maintain multiple non-volatile states are particularly promising for the realization of artificial synaptic devices. These multilevel states are essential for mimicking the complex behavior of biological synapses, allowing for more sophisticated and efficient information processing^{123–125}.

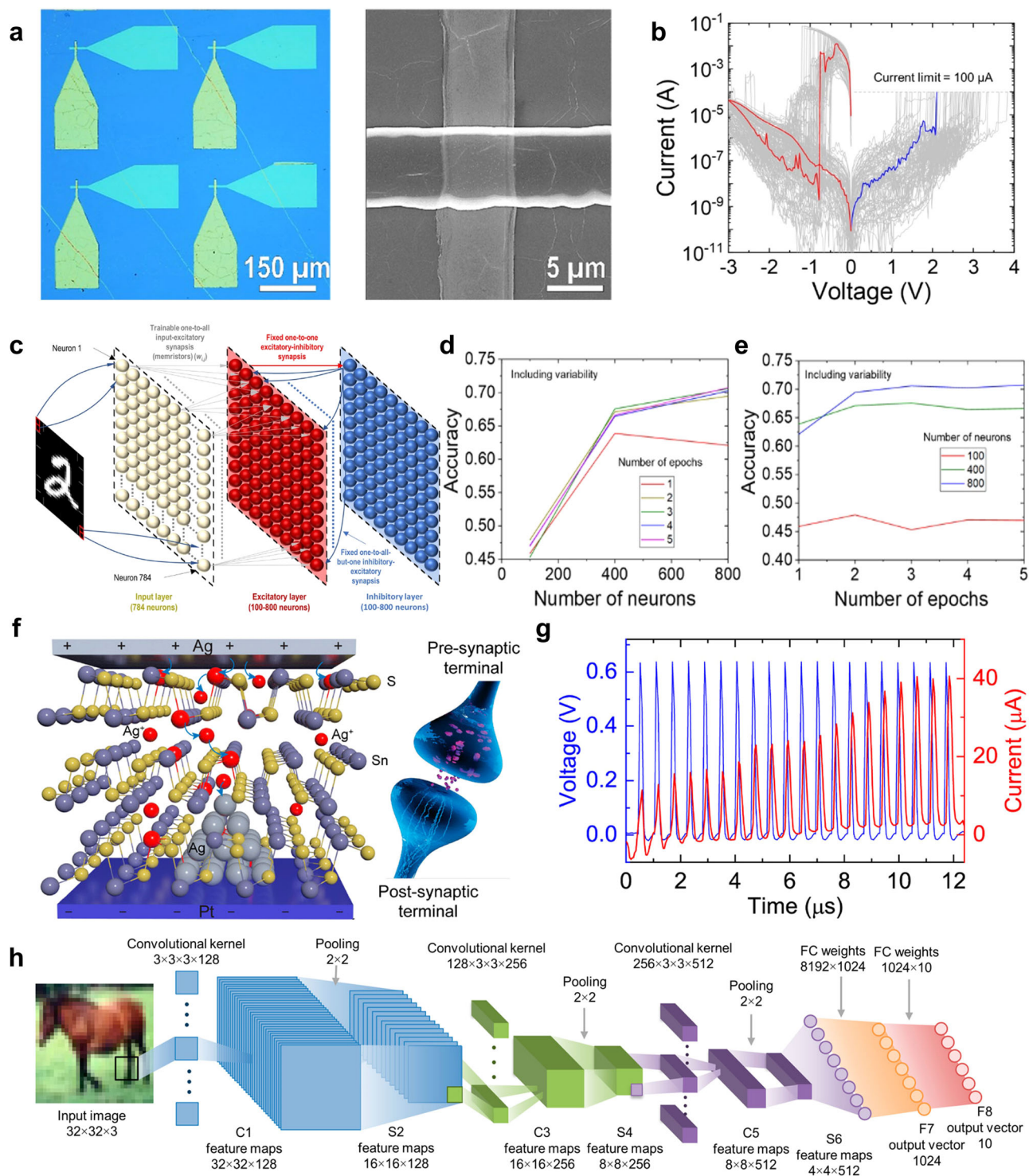


Fig. 4 | 2D memristor-based neural networks. **a** Optical microscopic and SEM image of the h-BN memristor. **b** *I-V* characteristics were measured across multiple resistive switching cycles, with compliance current set at $I_{CC} = 0.1$ mA. The graph illustrates 88 cycles of set (blue curve) and reset (red curve) processes. **c** SNN architecture. The input neurons (pre-neurons) are connected to every neuron in the excitatory layer (post-neurons). Each excitatory neuron is also connected to an inhibitory neuron, which exerts inhibition on all excitatory neurons except the one

from which it directly received input, illustrating lateral inhibition. Recognition accuracy for MNIST dataset versus the **d** number of neurons and **e** number of epochs. Reproduced with permission from ref. 113. **f** Schematic of Ag/Sn/Pt memristor. **g** Experimental data exhibiting short-term paired-pulse facilitation (PPF) with a pulse interval of 500 ns. **h** 8-layer VGG-8 convolutional neural network architecture used for CIFAR-10 image classification. Reprinted under terms of the Creative Commons license from ref. 115. Copyright © 2021 American Chemical Society.

The operation of 2D material-based memristors is often governed by mechanisms such as metal ion migration and structural phase changes^{90,126–128}. These mechanisms facilitate analog resistance switching in 2D material memristors, allowing them to effectively replicate different types of synaptic

plasticity, which is a fundamental feature of neural networks. This synaptic plasticity encompasses phenomena such as STP, LTP, and STDP. STP refers to transient increases in synaptic strength, while LTP involves more persistent changes that strengthen synaptic connections over time. STDP is a learning

rule that adjusts the strength of connections based on the precise timing of spikes between neurons. The ability of 2D material memristors to mimic these forms of plasticity renders them highly suitable for use in neuromorphic systems, where they can contribute to the development of brain-inspired computing architectures that are capable of learning and adaptation^{79,97,129,130}.

Advanced computing

In-memory computing

In the post-Moore's law era, the traditional von Neumann architecture has approached its maximum computational efficiency relative to energy consumption, causing a notable reduction in performance. Concurrently, the demand for computational power has escalated (especially in AI), highlighting that energy consumption is a critical issue. This has driven a movement toward energy-efficient computing, often called "green computing." In-memory computing presents a key approach to addressing these challenges by removing the necessity of data transfer between memory and the processing units, significantly reducing energy usage. By integrating memory and processing functionalities into a single unit, in-memory computing minimizes the latency and energy costs linked with data transfer, resulting in substantial improvements in computational efficiency. Neuromorphic computing was inspired by the functionality of the human brain and exemplifies the principles of in-memory computing. Neuromorphic systems can mimic the neural network architecture and its operational mechanisms, achieving remarkable levels of energy efficiency. These systems leverage SNNs and other brain-like computing models to process information in a highly parallel and energy-efficient manner^{130–132}.

Advances through 2D materials

The use of 2D materials has facilitated numerous advances in the field of in-memory computing. Researchers are redefining this era of computing by employing advanced architectures in memristor devices, encompassing single devices⁸ (Fig. 5a) and crossbar arrays¹³³ (Fig. 5b) for high-density memory and computing. Strategically engineered HSS enable self-selective memristor arrays³² (Fig. 5c), enhancing device performance and scalability. Furthermore, the development of 3D integration of memristor arrays has enabled three-dimensional fabrication¹⁰³ (Fig. 5d), contributing to high-density memory storage and extending beyond Moore's Law regarding chip fabrication. These advancements are revolutionizing the capabilities of neuromorphic computing, enabling more efficient and powerful data processing and storage solutions.

In 2018, Shi et al.¹³⁴ introduced a notable method by using multilayer h-BN as the resistive switching material, resulting in high-performance devices with dynamic response capabilities. Through modifications to the amplitude, duration, and frequency of electrical stimuli, they obtained a rapid (~200 μ s) and consistent relaxation across over 500 cycles with minimal fluctuations. This behavior can be ascribed to the resistive switching mechanism within the h-BN stack, which is then filled by metallic ions from nearby electrodes, creating boron vacancies. The power these devices use in standby mode can be as low as 0.1 fW, with 600 pW per transition and switching times of less than 10 ns, highlighting their potential for energy-efficient neuromorphic computing. The volatile and non-volatile properties of resistive switching were verified at the nanoscale using conductive atomic force microscopy (CAFM), highlighting excellent scalability potential, as illustrated in Fig. 5e–i. Li et al.¹⁰⁶ reported the development of an ultrathin heterostructure using 2D PdSeO_x/PdSe₂ for in-memory computing with a memristor array. This ultrathin heterostructure switching medium was developed through precise UV-Ozone treatment, effectively restricting the formation of conductive filaments. This resulted in highly uniform switching with low variability in set and reset voltages, specifically 4.8% and 3.6%, respectively. The device achieved five non-volatile states (Fig. 5j) with high linearity and symmetric analog weight updates by addressing compliance current. These tunable conductance states facilitated practical applications in image processing, as depicted in Fig. 5k.

Various 2D materials have been employed for in-memory computing and hardware security applications. For example, Xie et al.⁸ fabricated an h-

BN-based memristor array for both analog computing and ML hardware. Their study highlighted the hardware realization of dot product operations, which is a fundamental analog function that is frequently used in ML through the use of h-BN memristor arrays. The authors also showcased how a linear regression algorithm can be implemented in hardware using h-BN memristor arrays. A similar approach was demonstrated by Li et al.¹³³ by employing PdSe₂ for analog in-memory computing. Their study highlighted unusual resistive switching behavior featuring two distinct reset modes: total reset and quasi reset. In quasi-reset mode, switching variability in the memristors was reduced by a factor of six compared to the total reset mode. Additionally, these memristors demonstrated a low set voltage of 0.6 V, long retention times, and programmable multilevel resistance states. Sun et al.³² reported a unique and novel strategy using self-selective van der Waals HSS for creating large-scale memory arrays. The authors designed a self-selective memory cell featuring a vertical heterostructure composed of h-BN and graphene. This approach integrated non-volatile and volatile memory operations within the two h-BN layers, achieving a self-selectivity of 10¹⁰. The graphene layer played a crucial role in stopping the diffusion of volatile silver filaments, allowing for a novel integration of volatile and NVM processes.

Innovative architectures for enhanced performance

The exploration of hybrid architectures, such as the integration of 2D materials into traditional CMOS technology, has produced promising results. Sivan et al.³⁸ presented an innovative approach using a 1T1R RAM cell composed entirely of WSe₂ for 3D monolithic embedded memory. In this design, WSe₂ served as the active layer for both the transistor and memristor. The authors demonstrated a low-thermal-budget hybrid integration of 2D material-based 1T1R devices by employing a combination of solution-processed and exfoliated methods. Figure 6a presents a conceptual depiction of the 3D integration of CMOS logic and multiple layers of WSe₂ TFTs with ReRAM, outlining the thermal budgets for different levels. The ReRAM demonstrated non-volatile unipolar switching with voltages below 1 V and a low switching energy of 2.9 pJ per bit. This hybrid co-integration of TFT-ReRAM 1T1R enabled the creation of precise device-circuit models and facilitated the exploration of material-system memory cell co-design for advanced technologies. Zhu et al.¹³⁵ described hybrid 2D-CMOS microchips for memristive applications that incorporated an h-BN stack. In-memory computation was demonstrated through the construction of logic gates and the assessment of STDP signals, which are well-suited for SNNs. This development represented a major milestone in integrating 2D materials into microelectronic devices and memristive applications, as demonstrated by the exceptional performance and advanced technology readiness level achieved. Similarly, Feng et al.¹⁰⁸ introduced a multi-terminal mem-transistor crossbar array for in-memory computing that achieved enhanced programming parallelism by enabling the independent control of gates. This configuration facilitated in situ computation with a dense cell size ranging from 3 to 4.5 F² and a reduced sneak current to 0.1 nA. Furthermore, the system achieved a low switching energy of 20 fJ/bit at a voltage of 0.42 V. In addition, the architecture supported the multiply-and-accumulate operation, which is essential for pattern classification tasks, and demonstrated a high MNIST recognition accuracy of 96.87% due to its linear synaptic plasticity. Tang et al.¹⁰³ developed a wafer-scale solution-processed 2D MoS₂ memristor array for analog resistive memory-based computing. These memristors exhibited excellent endurance, long retention times, minimal device variation, and a significant analog on/off ratio with linear conductance updates. The diffusion of sulfur vacancies between the nanosheets was controlled by the distribution of flake sizes, modulating the switching characteristics. Additionally, the authors demonstrated a 3D memory cube by stacking 2D MoS₂ layers, advancing high-density neuromorphic computing systems.

Future directions and implications for AI

The previously mentioned advancements in neuromorphic and in-memory computing have profound implications for the development of AI and ML

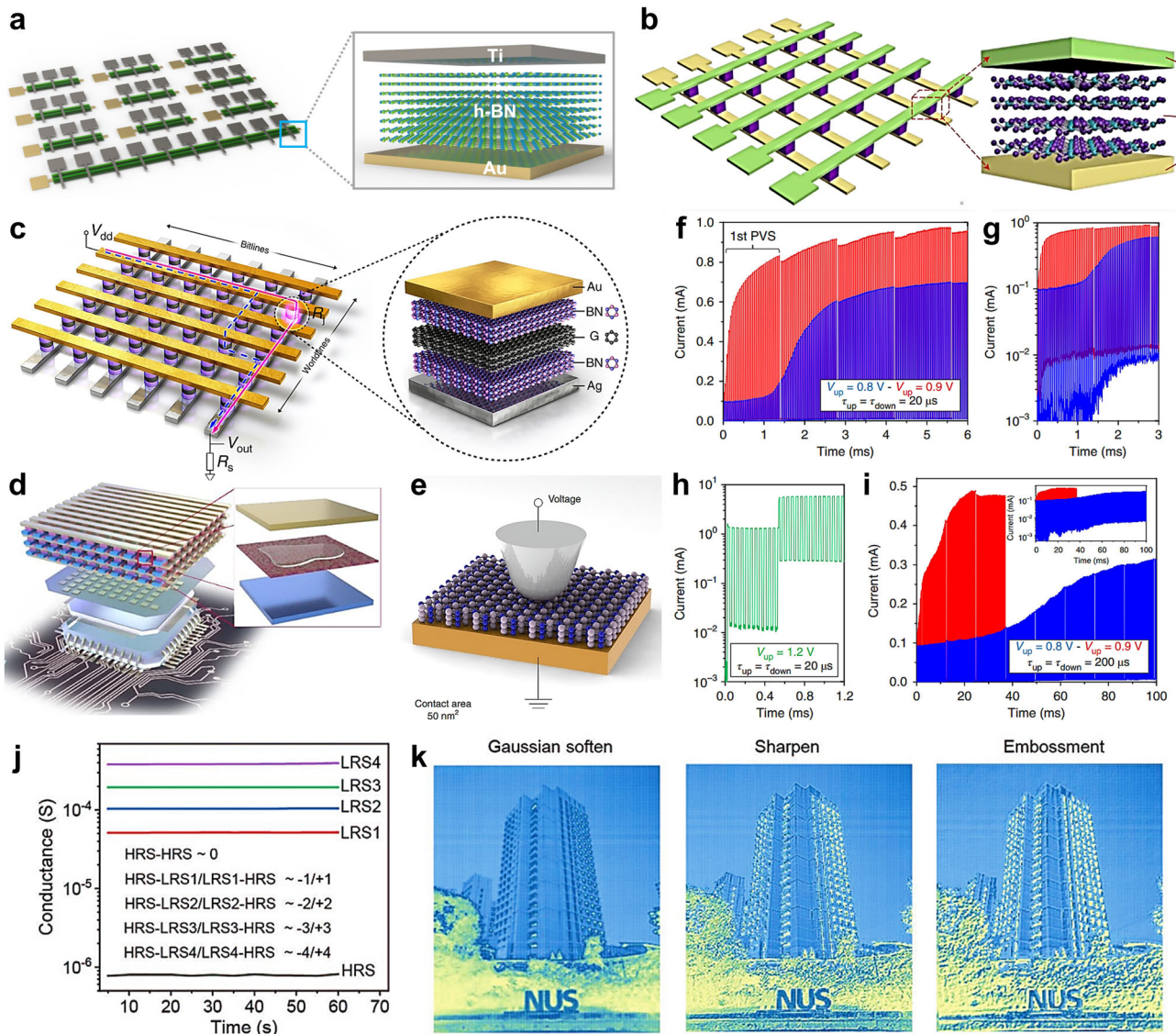
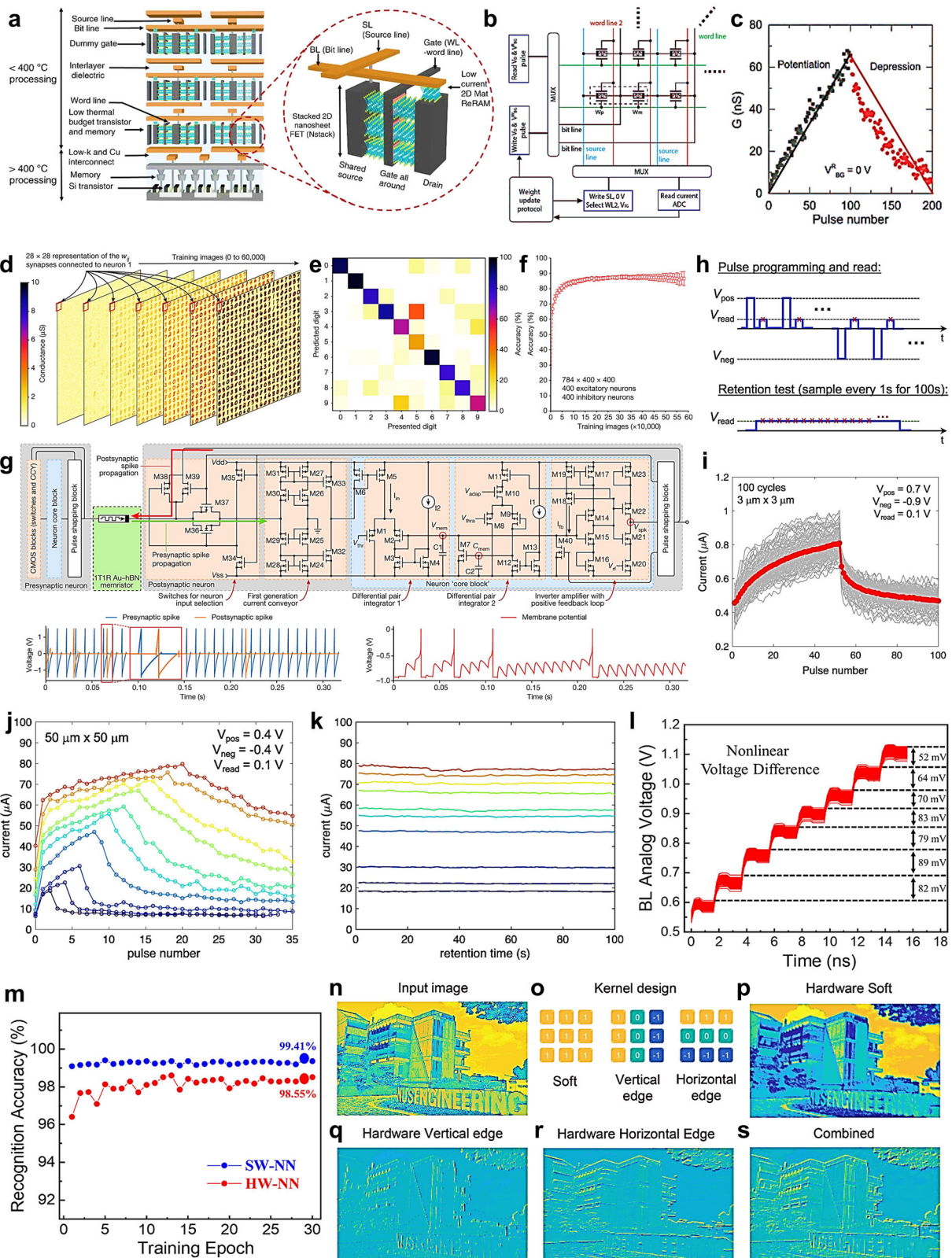


Fig. 5 | 2D memristor-based devices and architectures for in-memory computing. **a** Schematic of the arrays of Au/h-BN/Ti memristors and a graphical representation of a single Au/h-BN/Ti memristor, reproduced from ref. 8. **b** Crossbar for high-density memristor array, reproduced from ref. 133. **c** Self-selective memristor array achieved through heterojunction engineering with graphene and h-BN, reproduced from ref. 32. **d** 3D fabrication of memristor array for high-density chip functionality, reproduced from ref. 103. **e** Schematic of the CAFM experiments shows the tip/sample junction forming a nanoscale Pt/h-BN/Cu synapse. **f** Two sequences of 4 PVS (each with 30 pulses) observed in a $5 \times 5 \mu\text{m}^2$ 7-layer h-BN synapse, indicating

progressive synaptic potentiation. **g** Zoom-in of the current presented on a logarithmic scale. **h** A sequence of PVS with $V_{\text{up}} = 1.2 \text{ V}$, initially exhibiting an abrupt potentiation followed by an additional sudden increase in current, transitioning to the non-volatile RS regime. **i** Two sequences of PVS displaying synaptic potentiation, compared to that used in **f**, reproduced with permission from ref. 134. **j** By adjusting the compliance current, five distinct states are obtained, allowing for the mapping of weights within the range of -4 to $+4$. **k** Image-processing results using these five states, reproduced from ref. 106.

applications. Neuromorphic chips, which combine memory and processing elements, can perform complex computations with significantly lower power consumption compared to traditional architectures. This makes them particularly suitable for edge computing applications, where energy efficiency and real-time processing capabilities are paramount. Moreover, the synergy between in-memory computing and emerging materials (such as ReRAM) further enhances the potential of these technologies. These novel materials will enable the development of highly scalable and energy-efficient memory devices, paving the way for next-generation computing systems that can meet the ever-growing demands of AI and other data-intensive applications. 2D materials have several attributes that render them ideal for fabricating memristive devices, especially for use in device arrays. For example, the device thickness is significantly reduced to the sub-nanometer scale due to the monolayer structure of functional 2D materials,

facilitating outstanding scalability and precise control in fabricating high-density 3D crossbar arrays^{136,137}. To illustrate this point, researchers have engineered NVM devices using monolayer h-BN with an unprecedented thickness of just 0.33 nm^2 . Moreover, in memristor devices incorporating 2D materials (such as MoS_2), the extremely thin atomic layers enable precise gate control in multiterminal devices, improving the selection process within crossbar arrays¹³⁸. These factors of extreme thinness and control precision are crucial for developing compact and efficient memory storage solutions. Furthermore, it has been successfully demonstrated that many 2D materials (such as h-BN^{8,139} and MoS_2 ¹⁴⁰) allow large-area wafer-based fabrication and can achieve consistent thickness transfer. Recently, a method for wafer-scale growth of HfSe_2 was developed through the use of molecular beam epitaxy in conjunction with a metal-assisted van der Waals transfer process⁸⁰. These advanced fabrication and transfer techniques have



enabled the production of large-scale memristor crossbar arrays using 2D materials as functional components. This capability supports the mass production of high-performance devices necessary for practical applications.

The inherent attributes of 2D materials, such as a high surface-to-volume ratio and high carrier mobility, enhance their effectiveness in

memristive devices. The high surface-to-volume ratio enhances interactions between the material and the surrounding environment, which is beneficial for sensors and other responsive devices. The superior electronic properties, including high carrier mobility and tunable bandgaps, provide a versatile platform for designing devices with specific electronic characteristics. Finally, the layered nature of 2D materials, which is characterized by weak

Fig. 6 | 2D memristor-based architectures for in-memory computing.

a Conceptual depiction of 3D monolithic stacking with CMOS logic and WSe₂ TFTs with ReRAM, displaying the thermal budget. Reprinted under Creative Commons license from ref. 38. **b** Block diagram of the ANN hardware with dual-gated memristor crossbar synapses. Weight updates are achieved by pulsing bit lines (drain) and word line 1 (bottom gate), while word line 2 (top gate) helps to reduce sneak current. The dashed box shows two adjacent memtransistors with conductance levels w_p and w_m , storing a synaptic weight $w = w_p - w_m$. **c** Linearity of LTP and LTD in a dual-gated memristor synapse. Solid lines denote ideal responses. Reprinted under Creative Commons license from ref. 138. **d** Synaptic changes during training with 400 neurons. The red square highlights 784 synapses in a 28×28 grid. **e** Confusion matrix displaying the classification accuracy for each dataset category. **f** Classification accuracy variations with the number of training images, with error bars from 50 Monte Carlo simulations. **g** Circuit schematic of the neuron-synapse-neuron block integrating h-BN-based 1T1M cells with CMOS

circuitry. Colors differentiate the complete neuron (gray box), the core block (light blue box), and the individual building blocks (light red boxes). Reprinted under Creative Commons license from ref. 135. **h** Diagram of pulsed measurements and retention test. **i** Pulse programming for an Au/h-BN/Ti memristor, showing 100 cycles with positive and negative pulses. **j** Pulse measurement cycles with increasing the number of positive pulses from 2 to 20. **k** Retention characteristics right after applying the final positive pulse of each cycle shown in panel **j**. Reprinted under Creative Commons license from ref. 8. **l** Results from 1000 Monte Carlo simulations of an 8×8 crossbar array with 5% variations. **m** Graph of recognition accuracy for SW-NN and HW-NN across each training epoch. The highest accuracy achieved by SW-NN was 99.41%, while HW-NN reached 98.55%. Reprinted under Creative Commons license from ref. 140. **n** Original input image, **o** different kernel designs, **p-r** processed images with hardware using various kernels. Panel **q** combines results from **r** and **s**, displaying edge detection in both directions. Reproduced from ref. 80.

van der Waals interactions between layers and the absence of dangling bonds, promotes the formation of functional HSs and ensures efficient electrode contact in the design of memristive devices¹⁴¹. This property facilitates the integration of diverse materials to tailor the electronic properties of the device, enabling novel functionalities and improved performance. For example, creating HSs with graphene and TMDCs can result in devices with unique properties, such as high on/off ratios and excellent switching speeds. Overall, the unique attributes of 2D materials, such as their atomic-scale thickness, ability to form large-area uniform films, and compatibility with heterostructure formation, make them ideal candidates for next-generation memristive devices. These devices are expected to play a critical role in the development of high-density memory and logic circuits, offering potential solutions in various applications, including neuromorphic computing, data storage, and reconfigurable electronics. Importantly, research and development in 2D materials and their integration into memristive devices continue to drive innovation in nanoelectronics, paving the way for more advanced and efficient electronic systems.

Notable research has shown promising results. For example, Lee et al.¹³⁸ reported a notable dual-gate MoS₂ mem-transistor crossbar array, highlighting its potential for neuromorphic computing and data storage applications. The device demonstrated improved linearity and symmetry in LTP and LTD behavior, which were achieved through the dynamic tuning of learning rates using various V_{BG}^V and V_{BG}^R pulses (Fig. 6b). Figure 6c provides a detailed depiction of the hardware implementation of the ANN. The use of small grains in CVD-grown MoS₂ facilitated the development of mem-transistors with active channel sizes below 1 μm and a switching cycle energy consumption as low as 2 pJ. Zhu et al.¹³⁵ developed hybrid 2D-CMOS microchips that featured high integration density for memristors. The authors integrated multilayer h-BN onto the back-end-of-line interconnections of silicon microchips with CMOS transistors at the 180 nm technology node. The CMOS transistors provided precise current control across the h-BN memristors, resulting in an endurance of approximately 5 million cycles. This setup enabled in-memory computation, which was demonstrated through the creation of logic gates and the measurement of STDP signals (ideal for SNNs), as illustrated in Fig. 6d-g. Similarly, Xie et al.⁸ employed h-BN memristor arrays for analog machine-learning hardware. The authors fabricated and characterized Au/h-BN/Ti memristor arrays, as displayed in Fig. 6h-k, which were employed in dot-product operations. These memristor arrays exhibited excellent linearity and repeatability, which are essential for the development of ML hardware. This advancement represents a significant step forward in using 2D materials for ML hardware, highlighting the potential of h-BN memristor arrays to enhance the performance and efficiency of analog computation systems.

Additionally, Naqi et al.¹⁴⁰ developed a robust MoS₂ memristor array that was directly grown for application in in-memory deep-learning neural networks. This MoS₂ memristor functions as a synaptic device, exhibiting nearly linear synaptic behavior in terms of learning and forgetting. The device also displays both long-term and short-term memory dynamics by applying consecutive multilevel pulses with precise time durations.

Furthermore, the emulation of an artificial neural network using this synaptic device reached a recognition accuracy of 98.55%, which is only 1% less than that achieved with software-based neural network emulations (Fig. 6l, m). This work highlighted the potential of MoS₂ memristors to enhance the performance of deep-learning neural networks through hardware-based solutions. Li et al.⁸⁰ developed a large-scale HfSe₂-based memristor crossbar array for energy-efficient hardware using molecular beam epitaxy and a metal-assisted van der Waals transfer method. This memristor operated with a low voltage of 0.6 V and consumed minimal switching energy of 0.82 pJ. In addition, the device successfully emulated synaptic weight plasticity, demonstrating its potential for neuromorphic computing applications. Moreover, MAC operations with an error distribution as narrow as 0.29% and an exceptional power efficiency of over 8 trillion operations per second per watt were achieved. Additionally, the system demonstrated high recognition accuracy in ANN (Fig. 6n-s), suggesting its promise for advanced neuromorphic computing tasks.

In-sensory computing

As silicon-based transistors continue to shrink, creating more complex and energy-efficient circuits near sensory terminals becomes increasingly feasible. These circuits can preprocess sensor outputs, resulting in more efficient data transfer and processing^{142,143}. However, despite the significant reduction in redundant data provided by this near-sensor computing approach, physical separation remains between the sensors and computing units, which deteriorates the speed and energy efficiency¹⁴²⁻¹⁴⁴. To address this issue, integrating computing functions directly into sensors can effectively eliminate the physical divide, enabling a paradigm shift toward in-sensor computing. In this approach, external stimuli are converted into electrical signals by sensors, allowing for efficient processing right at the point of data collection¹⁴⁴⁻¹⁴⁶.

Integrating computing capabilities within sensors enables real-time data processing at the point of data collection, enhancing the responsiveness and efficiency of the system. This approach minimizes the latency and energy consumption associated with data transmission between the separate sensing and processing units. Furthermore, in-sensor computing can pave the way for advanced applications in areas such as neuromorphic computing, where sensory data is processed similarly to biological neural networks, offering potential breakthroughs in AI and ML¹⁴⁴. The ongoing advancements in nanoscale transistor technology and materials science are crucial for the development of in-sensor computing systems. Emerging technologies, such as 2D materials and flexible electronics, hold significant promise for creating highly integrated, multifunctional devices. These advancements could result in a new generation of smart sensors with enhanced capabilities, improved energy efficiency, and reduced form factors, driving innovation across various fields, from healthcare to environmental monitoring.

Lin et al.¹⁴⁷ explored the use of CeO₂/MoS₂ HSs to create a bionic visual system with nociceptive sensing capabilities. The authors developed an optoelectronic memristor from these HSs, enabling adjustable

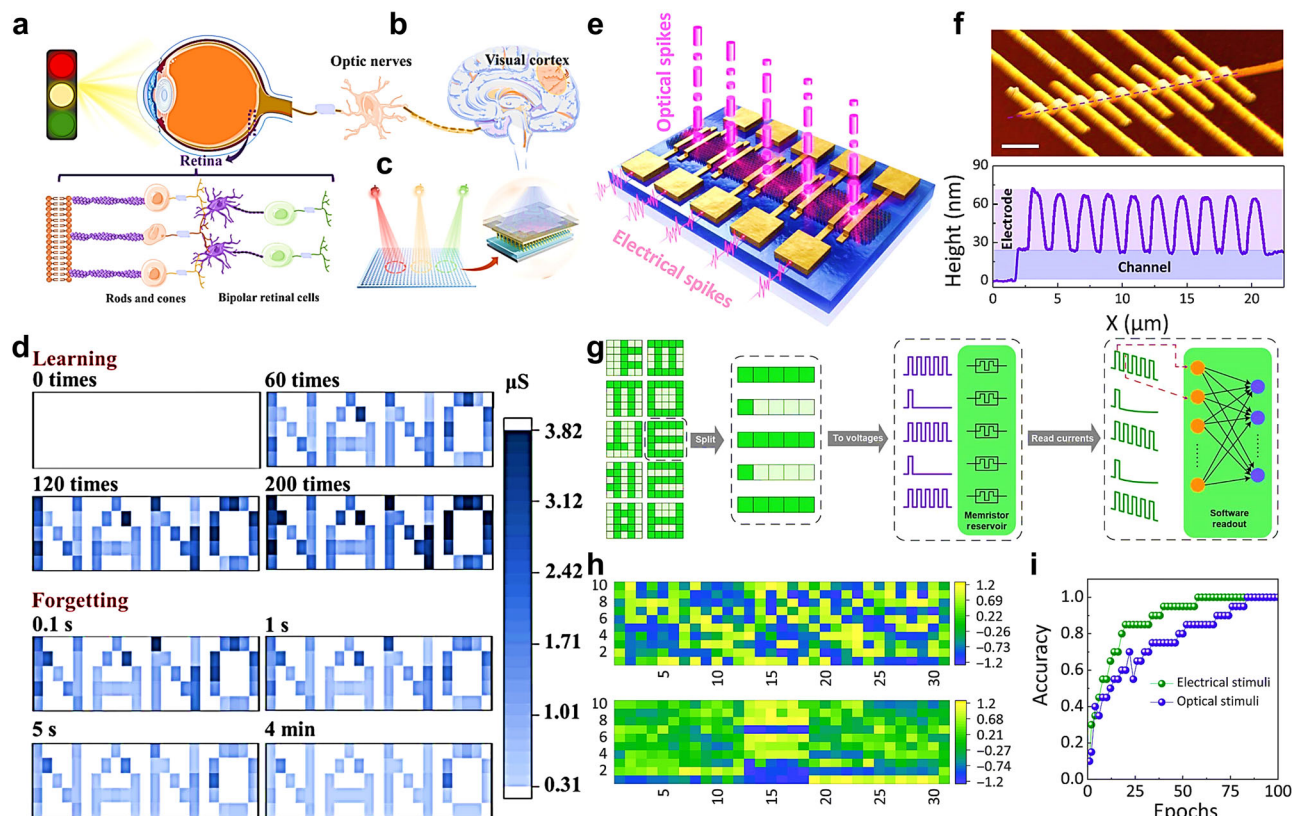


Fig. 7 | In-sensory computing. **a** Biological visual system comprising the retina, optic nerves, and visual cortex. **b** Diagram displaying key functional cells in the retina, such as rods, cones, and bipolar retinal cells. **c** Diagram of the artificial visual array with optoelectronic memristors and a circular shadow mask on top. **d** “NANO” pattern used to demonstrate short-term and long-term memory behavior in synapses. Reprinted under terms of the Creative Commons license from ref. 147. **e** Multifunctional memristor array responsive to both electrical and optical inputs. **f** AFM image and corresponding line profile of the device array utilized in the

research, with a scale bar of 2 μm . **g** Operation of an optoelectronic RC system employing 2D SnS memristors for distinguishing consonants and vowels in the Korean alphabet. The array of five memristors was stimulated using temporal pulse sequences. **h** Weight distribution in the readout layers after 100 epochs of applying electrical and optical stimuli. **i** Progression of classification accuracy rates through standard batch gradient descent over 100 epochs of in situ training for electrical (depicted in green) and optical (depicted in blue) stimuli. Reprinted under terms of the Creative Commons license from ref. 95.

optoelectronic synaptic functions. This advancement resulted in a multifunctional artificial visual system that supports electrical storage, light sensing, memory, and visual nociception. This device exhibited a strong response to both UV and visible light, demonstrating high photosensitivity and light-induced synaptic functions. Additionally, it features sophisticated mechanisms for transitioning between short and long-term memory (STM/LTM), as well as for managing learning, forgetting, and relearning by adjusting the light intensity and duration, as displayed in Fig. 7a–d. In another study, Sun et al.⁹⁵ demonstrated in-sensor reservoir computing (RC) for language learning using SnS flakes and successfully implemented a novel in-sensor RC system with dual-mode operation, as depicted in Fig. 7e, f. The integrated SnS-based memristors exhibited unique and opposite electrical and optical response trends, effectively generating high-dimensional states in the optoelectronic RC system to manage complex spatiotemporal input signals (Fig. 7g–i). The system attained a notable accuracy rate of 91% when classifying five real Korean sentences, even when these sentences included deliberate noise. Such energy-efficient methods enhance ML applications with temporal inputs at the edge, marking a significant advancement for the Internet of Things (IoT) era.

Semiconductors with bandgaps within the visible light spectrum, such as WSe_2 , MoS_2 , WS_2 , and SnS are highly effective for use in photodetectors within sensors. These materials exhibit excellent photosensitivity, which has been successfully integrated with memristive circuits to create unified sensor-processor devices. Moreover, the properties of these semiconductors can be leveraged to design devices that combine sensing and processing functions^{148–150}. The switching mechanisms in these materials involve the

incorporation of oxygen, which heals sulfur vacancies and restores the material’s original resistance state. This reversible switching mechanism, driven by light and environmental conditions, underscores the potential of 2D materials in developing advanced photodetectors and memory devices. By combining photosensitive materials with memristive circuits, it becomes possible to design compact, energy-efficient devices that can sense and process optical information directly—an especially beneficial capability for applications in AI where real-time data processing is critical. The use of 2D materials such as WSe_2 ⁷³, MoS_2 ¹²⁶, WS_2 ¹⁵¹, SnS¹⁵⁵, and Sb_2S_3 ¹⁵² in photodetectors and memristors opens up new possibilities for the development of multifunctional devices. In addition, the unique properties of these materials, including a high surface area, tunable bandgap, and excellent electronic characteristics, make them ideal candidates for next-generation sensor-processor systems. Ongoing research and development in this field are expected to result in further innovations that will enable more efficient and versatile electronic devices.

WSe_2 and WS_2 are stable semiconductors with direct bandgaps that are well-suited for absorbing visible light, making them excellent choices for applications in photodetectors and optoelectronic devices^{28,153}. Their stability and efficient light absorption properties position these materials as key components in advanced sensor technologies. Recent advancements by Wang et al. demonstrated how a retinomorph sensor could be built using WSe_2 . In their approach, the photoresponses were used to manage a gate terminal in a memristive device, allowing for image data processing directly within the sensor²⁸. This approach exemplifies how 2D materials can be used to integrate sensing and processing functions, enhancing the efficiency and

functionality of optoelectronic systems. WSe_2 exhibits impressive nonlinear optical properties, which have been leveraged in the development of nonlinear transistors. For example, Tong et al. successfully combined WSe_2 with lithium niobate to produce nonlinear transistors and NVM devices that exhibit enhanced performance¹⁵⁴. This integration highlights the versatility of WSe_2 in creating advanced electronic components that can perform complex functions. Furthermore, WSe_2 mem-transistors have been integrated into circuits to enable hyperbolic tangent and sigmoid activation functions in artificial neurons, as demonstrated by Sebastian et al.¹⁵⁵. This innovation highlights the potential of WSe_2 -based devices in neuromorphic computing, where they can replicate the behavior of biological neurons for more efficient data processing and learning. Additionally, SnS is recognized as a layered semiconductor with outstanding optical sensitivity, broadening its potential applications in optical and electronic technologies. This sensitivity originates from the high number of defect states arising from vacancies in both tin (Sn) and sulfur (S). These defect states contribute to the exceptional photosensitivity of SnS, rendering it suitable for optoelectronic applications. Sun et al. recently made notable progress by developing an SnS-based memristor array that was specifically designed for language learning applications⁹⁵. Similarly, vapor transport deposited (VTD) Sb_2S_3 -based multilevel memristor devices with optically controllable functionalities have been explored, exhibiting higher stability and reliability across the devices¹⁵². Within this configuration, the memristor undergoes direct stimulation by optical signals, effectively leveraging the defect states present within the bandgap to modulate the resistance of the device. The SnS memristor array operates in dual mode, responding to both optical and electrical stimuli. This capability is enabled by the existence of donor and acceptor states within SnS, enabling simultaneous processing of optical and electrical inputs. This dual-mode operation is particularly advantageous for applications requiring simultaneous handling of multiple types of signals, such as in advanced sensor networks and cognitive computing systems.

Photon responses in 2D materials (such as graphene and MoS_2) have been harnessed to create optoelectronic memristive devices. These materials exhibit strong photoresponsivity, where light exposure can induce changes in resistance, enabling the integration of optical and electronic functionalities^{34,95,153}. This property is particularly advantageous for applications in photonic computing and optoelectronic memory. The unique properties of WSe_2 , WS_2 , and SnS, including their direct bandgaps, stability, and sensitivity to light, make them ideal materials for photodetectors and optoelectronic applications. This integration of materials into memristive devices and circuits has enabled the development of multifunctional components that are capable of sensing, processing, and learning. As research in this field progresses, these materials are expected to play a crucial role in the advancement of next-generation electronic and optoelectronic technologies.

Hardware security

PUF

In the rapidly evolving landscape of cyber security, the need for robust tamper-resistant authentication mechanisms has become increasingly critical. Traditional authentication methods, such as passwords, biometric systems, and cryptographic keys, have vulnerabilities that can be exploited by increasingly sophisticated cyber-attacks. Accordingly, researchers are exploring innovative solutions that leverage the inherent physical properties of materials and devices to enhance security. One such promising technology is the physical unclonable function (PUF)⁴⁷.

Memristor-based weak PUFs

Weak PUFs are primarily used to create and safeguard encryption keys. Unlike strong PUFs with many challenge-response pairs (CRPs), weak PUFs have fewer CRPs and improved reliability. One way to implement a weak PUF is through memristor-based systems by using switching parameters^{156,157} and device-to-device (D2D) variations^{158–160}. In the context of memristor-based weak PUFs, these systems leverage the unique properties of memristors, which are electronic devices that are capable of altering their resistance based on the applied voltage. By harnessing switching

parameters and D2D variations within memristor arrays, weak PUFs can be effectively implemented. When considering a weak PUF based on switching probability, a specific program is executed when the switching probability reaches 50% across the entire array. This program randomly assigns the devices within the array to either “0” or “1” states, contributing to the generation of cryptographic keys. However, it should be noted that this method is more suitable for smaller arrays due to challenges such as the voltage drop (IR drop) effect that occurs in larger arrays. This effect can impact reliability, particularly concerning variations from one cycle to another C2C.

In larger memristor arrays, determining the appropriate program voltage also becomes a complex task. This voltage is derived statistically from a multitude of devices within the array, adding a layer of complexity to the implementation process. In contrast, a D2D variation-based approach in weak PUFs involves leveraging the inherent variations between individual memristor devices. These variations are known as D2D variations and are harnessed to enhance the uniqueness and unpredictability of the generated keys, improving the security of the cryptographic system. However, weak PUFs based on memristor technology offer a robust solution for generating and protecting encryption keys, with considerations of array size and reliability challenges while leveraging variations within memristor devices to ensure cryptographic security. Woo et al.¹⁶¹ investigated the use of a $\text{CuTe}_2/\text{HfO}_2$ heterostructure in heterojunction memristors for developing tunable stochastic devices aimed at energy-efficient encryption and computing. Their findings indicated that these $\text{CuTe}_2/\text{HfO}_2$ memristors could produce genuinely random and physically unclonable functions under certain operational biases. For example, under different biases, the memristors were capable of executing universal Boolean logic operations. This research demonstrated the ability of a single system to perform cryptographic key generation, universal Boolean logic functions, and encryption/decryption tasks (Fig. 8a, b).

Memristor-based strong PUFs

Strong PUFs are used for verifying identities and require each CRP to be distinct, resulting in the need for an extensive CRP space, which can affect reliability. Traditional CMOS-based strong PUFs often use time-delay circuits, such as arbiter or ring oscillator PUFs. However, implementing these structures with memristors is challenging due to the need for complex circuits for operations such as forming, reset, and set. A simpler method for memristor-based strong PUFs involves randomly selecting two cells from an $M \times N$ memristor array and using their comparison as the response^{162–164}. This method can generate up to $C_{M \times N}^2$ bits of response, providing a large CRP space with sufficiently large arrays. Most memristor-based strong PUFs follow this principle (or its variants), while others use more complex techniques such as memristor-based arbiters or ring oscillator PUFs. However, these methods often require numerous devices and exhibit strong CRP correlations^{164–166}. To overcome these issues, a common approach for memristor-based PUFs involves leveraging the analog state and nonlinear conductance variations in the integrated memristors. This innovative method enhances the performance of memristor PUFs by analog tuning of the memristors' conductance. However, 2D materials are much less explored for this application under strong PUF domains. Therefore, exploring 2D materials could open new possibilities for enhancing the performance and scalability of PUFs in terms of identity authentication.

True random number generators (TRNGs)

True random number generators (TRNGs) are a fundamental pillar of ensuring information security and are used extensively in security chips and encryption algorithms. Conventional TRNGs primarily depend on random noise produced within CMOS digital and analog circuits, including sources such as thermal and shot noise. However, despite the recent advancements in CMOS-based TRNGs, they exhibit several shortcomings, including the masking of random noises by deterministic disturbances due to their lower amplitude. This results in a larger bias towards “1” or “0” in the raw output. Additionally, the smaller noise amplitude necessitates complex preamplifier circuits for effective use. Recently, memristors have become strong

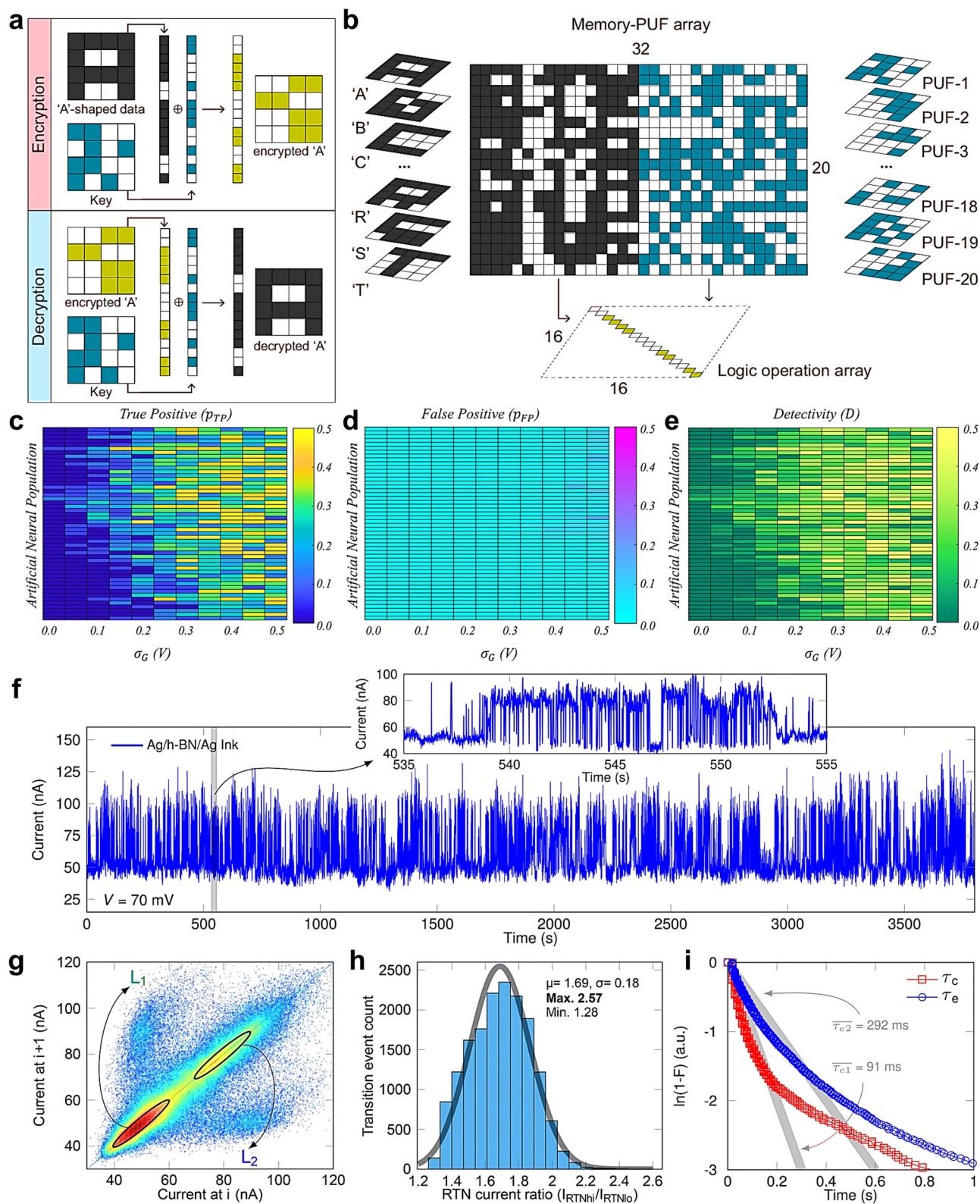


Fig. 8 | Hardware security. **a** Encryption and decryption of A-shaped data are carried out using a key equivalent to PUF 1, with the process executed through an XOR operation following the DC logic scheme. **b** 20×32 hybrid mem-PUF arrays utilized for encryption, with permission for ref. 161. Colormaps of the likelihood or probability of **c** true positive, **d** false positive, and **e** detectivity as a function of for $P = 50$ encoders. Reproduced with permission from ref. 168. **f** RTN current through an Ag/h-BN/Ag-ink memristor device measured under a constant low applied voltage of 70 mV. The signal remains stable for over 1 h, the longest duration reported for a 2D material-based device. The inset details 20 s of data, demonstrating a high on/off ratio

(greater than 2) and short capture and emission times, reflecting an RTN signal of exceptional stability. **g** Weighted time lag plot of the RTN trace in panel **f**. **h** Histogram displaying the ratio of currents before and after an RTN transition, determined by dividing the high current (I_{RTNhi}) by the low current (I_{RTNlo}). The curve represents a Gaussian fit to the data, with a mean value of $\mu = 1.69$. The highest transition ratio observed was 2.57. **i** Exponential distribution of τ_c and τ_e values is plotted for the entire dataset shown in panel **f**. Transitions where $\ln(1 - F) > -2$ occur within 400 ms for 87% of the cases. The gray thick lines indicate the average values of the bimodal exponential distributions. Reproduced from ref. 169.

candidates for hardware security solutions due to their inherent characteristics of true randomness, especially in TRNG applications. Memristor-based TRNGs leverage various phenomena, such as conductance-to-conductance (Cn2Cn) variations, switching probability, and random telegraph noise (RTN) in memristive devices. Among these approaches, Cn2Cn variation-based TRNGs offer an unbiased output without the need for additional circuits to adjust the bias, while RTN-based TRNGs can operate without preamplification circuits due to the significant amplitude of RTN¹⁶⁷.

Dodda et al.¹⁶⁸ presented a bioinspired low-power crypto engine designed for near-sensor security using 2D mem-transistors. Their study demonstrated that the encrypted information remains secure against eavesdroppers with limited resources while having access to deep neural networks. The hardware setup included 320 monolayer MoS₂-based mem-transistors, each operating with energy consumption in the picojoule range while providing enhanced security close to the sensor. This innovative use of MoS₂ mem-transistors would be applicable for computing, storage, and sensing applications. This encrypted data has been demonstrated to be resistant to adversaries employing advanced ML techniques, including trained DNNs (see Fig. 8c–e). Pazos et al.¹⁶⁹ showcased the hardware implementation of a TRNG by combining h-BN memristors with a commercial microcontroller. A key aspect of their work was the stability of the h-BN memristors, which exhibited highly stable RTN signals for extended periods (>1 h) while maintaining low power consumption (~650 nW) (Fig. 8f–i). These findings mark a significant advancement toward the development of sophisticated TRNG circuits that would be ideal for IoT applications. Additionally, this work illustrates the potential for integrating 2D materials with conventional electronics, leveraging the advantages of both to enhance performance. Similarly, Wen et al.¹⁷⁰ reported advanced data encryption by employing 2D materials, focusing on the fabrication of highly stable TRNG circuits. Circuits constructed from MIM devices with multilayer h-BN exhibit low power consumption, maintain high randomness (even for extended bit strings of up to 224 – 1 bits), and achieve a throughput of 1 Mbit/s. These features collectively highlight the potential of multilayer h-BN MIM devices creating efficient and reliable TRNG circuits for advanced data encryption. However, switching probability-based TRNGs faces challenges related to device endurance, particularly due to the specific pulse width and voltage combinations required for a 50% success rate per write cycle. Recent research has made advances in addressing these issues by selecting suitable memristive devices. Additionally, exploring various stochastic behaviors has resulted in innovative TRNG designs. Notable examples include TRNGs that use current differences with fractional stochastic models and those that use write delay times in diffusion memristors. Several significant advancements in this area include a TRNG that exploits RTN characteristics, another that employs different currents based on a fractional stochastic model, one that relies on Cn²Cn variation, and a TRNG that takes advantage of write delay times in diffusion memristors^{171–173}. These advancements showcase the versatility of memristor-based TRNGs and highlight ongoing efforts to enhance randomness and reliability in hardware security implementations.

Recent research has explored RTN-based TRNGs, aiming to leverage the inherent stochastic nature of memristors for generating high-quality random sequences^{167,174–176}. Traditional TRNGs measure the voltage across a device at a clock signal and compare it to a fixed reference voltage to produce random values. However, controlling the frequency and amplitude of RTN in memristors is challenging, making it difficult to achieve a stable and unbiased output. The new RTN-based TRNG innovative approach addresses the limitations of existing methods by combining the strengths of two distinct designs: a CMOS-based timing jitter TRNG and a conventional RTN-based TRNG¹⁷⁷. The timing jitter phenomenon originates from thermal noise in a ring oscillator and has been used previously to generate randomness. However, relying solely on this method to generate adequate randomness has been challenging, often requiring additional complex peripheral circuits (such as feedback shift registers and logic gates).

Leveraging hardware primitives that possess inherent stochastic behavior at the physical level is a highly promising method of generating

truly unpredictable random numbers¹⁷⁸. Within the field of nanoelectronics, memristive TRNGs are notable for their significant variability and high entropy. Moreover, memristive TRNGs based on 2D materials have demonstrated exceptional performance, which is attributed to their unique lattice structures. For instance, Wen et al.¹⁷⁰ created an advanced data encryption system by leveraging a stable RTN signal from a well-crystallized h-BN memristor. This innovative fusion of memristor technology with established TRNG principles represents a promising direction in terms of advancing hardware-based random number generation for diverse applications in security and cryptography. The ongoing development of high-speed TRNG designs based on memristor technology represents a crucial advancement in hardware security. These designs are particularly well-suited for applications requiring rapid processing and high-frequency operations. By capitalizing on the unique characteristics of paired memristors and their Cn²Cn variations, these TRNG designs offer robust and efficient solutions to meet the stringent security demands of contemporary technologies. A comprehensive overview of in-memory computing, in-sensory computing, and hardware security is detailed and summarized in Table 3.

Integrating technology

Complexity and memristor adaptation

Future advancements in computing performance should incorporate the dynamic and adaptive features found in natural and biological systems. Biological systems, at all scales (from molecular to organismal scale), demonstrate an intrinsic ability to respond to their environment and historical stimuli. For example, basic molecular systems (such as nucleic acids) demonstrate adaptive behaviors (including replication and self-repair) in response to local environmental conditions. At a higher level of complexity, neurons, which are the primary information-processing units in biological systems, display over 20 different dynamical behaviors that are influenced by their electrochemical history and environmental stimuli. This adaptability extends to more complex systems, including the eye, the immune system, and even entire organisms. Here, functional complexity and adaptive capacity increase proportionally with organizational complexity. In stark contrast, modern computing systems are predominantly built on static elements that are characterized by zeroth-order complexity. However, these systems lack an inherent ability to adapt and respond dynamically to changing conditions, limiting their potential to reach the levels of efficiency and functionality observed in biological systems. To bridge this gap, future advancements in computing must incorporate elements that emulate the adaptability and responsiveness of their biological counterparts. Such bio-inspired computing systems would leverage adaptive algorithms and dynamic architectures to respond in real-time to environmental inputs and historical data, potentially revolutionizing fields ranging from AI to neuromorphic engineering. Embracing these principles could result in the development of robust, efficient, and highly adaptive computing systems that parallel the sophistication and resilience of natural biological processes.

The pivotal role of memristors

Memristors have emerged as a pivotal element in the quest for enhancing computing complexity, particularly in bio-inspired computing paradigms. Conventional approaches in bio-inspired computing have often aimed at replicating basic biological functions, primarily employing transistor-based circuits (such as CPUs and GPUs) to model a range of dynamic systems. However, the advent of memristors has significantly simplified this approach. Memristors were initially theorized in 1971 and physically realized in 2008, representing electrical circuit elements embodying at least one state equation and introducing at least first-order complexity into computing systems. Incorporating state equations in memristors results in history-dependent behaviors in current-voltage plots, offering volatile and NVM effects.

Non-volatile memristors serve as excellent candidates for electrical synapses due to their tunable weight and NVM characteristics, rendering them ideal for conductance-weighted input-output transformations. In

Table 3 | Summary of memristor devices based on 2D materials for in-memory and in-sensory computing

Device structure	Switching type	Stimulus type	Conductive states	Simulation	Applications	Ref.
Au/Ti/h-BN/Cu	Bipolar	Electric	-	-	Neuromorphic computing	134
Ti/Au/MoTe ₂ /Ti/Ni	Bipolar	Electric	-	-	Neuromorphic computing	197
Al/AIO _x / Graphene	Bipolar	Electric	60	-	Neuromorphic computing	198
Bi ₂ O ₂ Se three terminal memristor	Bipolar	Electrical	10	Yes	Neuromorphic computing.	199
Al/MoS ₂ /MoO _x / ITO	Bipolar	Electric + Optical	4	-	In-sensory computing	200
Au/TiO _x /Gr/Au	Bipolar	Electric	-	-	1S1M	201
Cu/MoS ₂ /Au	Bipolar	Electric	20	-	Neuromorphic computing	126
MoS ₂ /hBN 1T1R	Hybrid	Electric	30	-	In-memory computing	202
Al/AIO _x /graphene/SiO ₂	Hybrid 1T1R	Electric	-	-	Gate controlled memory	71
Ag/WO _{3-x} /WSe ₂ /Au	bipolar	Electric	30	-	Neuromorphic computing	196
Ti/Au/MoS ₂ /Ti/Au	Bipolar	Electric	100	-	In-memory computing	203
Au/MoS ₂ /Au/SiO ₂ /Si	Hybrid	Electric	10	-	In-memory computing	29
Au/WO _{3-x} /Ti	Bipolar	Electric	50	Yes	In-memory computing	204
Au/ Li _x MoS ₂ /Au/SiO ₂ /Si	Hybrid	Electric	100	-	In-memory computing	205
Au/SnO _x /SnSe/SnO _x /Au	Bipolar	Electric	3	Yes	Multi-level computing	206
Au/BN/G/BN/Ag	Bipolar	Electric	3	-	In-memory computing	32
Ti/Au/MoS ₂ /Ti/Au/SiO ₂ /Si	Hybrid	Electric + Optical	-	-	In-sensory computing	207
Au/MoS ₂ /h-BN/AU	Bipolar	Electric + Optical	-	-	In-sensory computing	208
Cu/h-BN/Au	Bipolar	Electric	-	-	In-memory computing	134
Ti/PdSeO _x /PdSe ₂ /Au	Bipolar	Electric	100	Yes	In-memory computing	106
Au/WSe ₂ /Wo _x /Au	Bipolar	Electric	-	-	In-memory computing	38
Au/MoS ₂ /Au/SiO ₂ /Si	-	Electric	100	Yes	In-memory computing	138
Au/h-BN/Au	Bipolar	Electric	-	Yes	In-memory computing	135
Au/h-BN/Ti	Bipolar	Electric	100	Yes	In-memory computing	8
Ag/MoS ₂ /Pt	Bipolar	Electric	20	Yes	In-memory computing	140
Au/HfSe ₂ /Au	Bipolar	Electric	100	Yes	In-memory computing	80
Ag/CeO ₂ /MoS ₂ /ITO	Bipolar	Electric + Optical	1000	Yes	In-sensory computing	147
Au/SnS/Au	-	Optical	-	Yes	In-sensory computing	95
CuTe ₂ /HfO ₂ /Pt	Bipolar	Electric	-	Yes	Encryption & computing	161
Au/MoS ₂ /Au	-	Electric + optical	-	Yes	Crypto engines & sensor security	168
Ag/h-BN/Ag	Bipolar	Electric	-	-	TRNG	169

contrast, volatile memristors exhibit non-linear transformations, making them suitable for thresholding and electrical neuron emulation functions. Moreover, volatile memristors can generate complex temporal dynamics similar to higher-order neuronal behaviors. Unlike transistor-based hardware that requires multiple devices to simulate biomimetic functions, memristors inherently embody simple biomimetic functions, resulting in more efficient bio-inspired computing systems. Although the exploration of memristors with higher-order complexity is in its early stages, recent research has indicated the potential to engineer qualitatively complex behaviors (particularly biomimetic) from electro-physical-chemical processes within memristors. This capability allows a single memristor device to replace hundreds or thousands of transistors, resulting in enhanced system-level complexity and energy efficiency, which is a fundamental principle underpinning complexity in computing, especially in the field of bio-inspired computing.

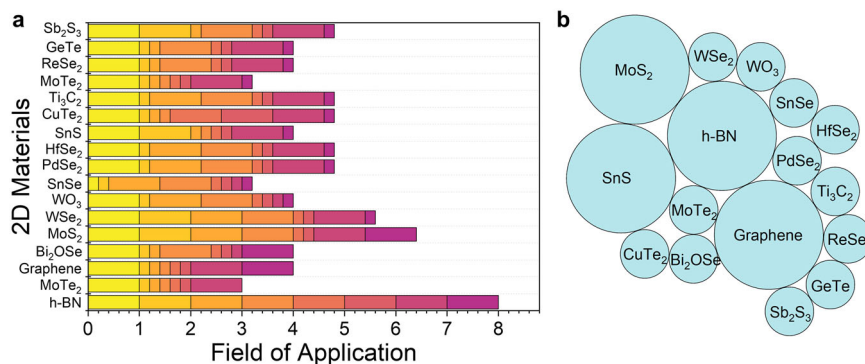
The growing interest in memristors stems from their multidisciplinary potential across various applications, including neuromorphic computing, data storage, and advanced signal processing. Incorporating 2D materials into the design of memristors is particularly promising due to their unique properties, which can enhance device performance and expand operational capabilities. However, a review of the literature over the past decade reveals the concerning trend that only a limited number of 2D materials, primarily h-BN and MoS₂, have been extensively studied for their potential in

memristor technology beyond memory applications (Fig. 9a). While these materials show promise in various domains, many other 2D materials with unique properties remain underexplored. This is especially notable in critical areas such as encryption, TRNG, and PUFs, which are increasingly important for secure data transmission and hardware security. The underutilization of these materials presents significant opportunities for further research, as portrayed in Fig. 9b. For instance, TMDCs and other 2D materials could introduce novel mechanisms for resistance switching, potentially leading to devices with enhanced performance metrics, such as lower energy consumption, faster switching speeds, and improved scalability. Expanding investigations into these lesser-explored materials could unlock new functionalities that enhance the impact of memristor technology in emerging fields, facilitating the development of advanced applications that leverage the unique properties of various 2D materials and driving innovation in both academic and industrial domains.

Integrating technologies for computing advancement

Large-scale sensor arrays must be integrated into modern silicon technology to enable practical in-sensor computing. As information processing demands increase across various fields, in-sensor computing requires more specialized units. Hence, for efficient and compact processing systems, sensor units, array layouts, and peripheral circuits should be co-designed. One challenge is integrating sensors with selective cells, especially in large

Fig. 9 | Overview of 2D materials applications. **a** benchmarking of various 2D materials alongside their respective applications: 1. Neuromorphic computing, 2. In-sensory computing, 3. In-memory computing, 4. Multilevel computing, 5. Encryption data, 6. RNG/PUF, 7. Artificial Synapse, 8. CMOS integration. **b** Schematic illustration of widely used 2D materials in the memristor domain, emphasizing their roles beyond traditional memory applications.



arrays. Furthermore, the structures must be compatible with high performance. Typically, individual sensors are accessed element by element. A one-transistor-one-sensor configuration enables access by activating the corresponding transistor. Two-terminal selectors with intrinsic nonlinearity are smaller and better for high-density integration. However, using three-terminal transistors instead improves reliability at the cost of density. Thus, the trade-off between performance and integration density is critical. Array-level design depends on the desired computing functions. Unlike conventional layouts, in-sensor computing, layouts must consider the interactions between environmental stimuli and sensing units. Preliminary computing functions in the sensor array reduce the need for certain peripheral units. However, array outputs still need complex processing for tasks such as object recognition, requiring both neural networks and analog-to-digital converters. The number of outputs equals the sensory nodes, increasing the need for post-processing units as the array size grows. Interconnecting sensors and physical coupling can reduce the number of output nodes. Moreover, multiplexing strategies can further decrease the number of post-processing units, although this would cause slower information processing. Shared interconnections improve precision by reducing resistance variation at the nanoscale. These trade-offs must be carefully considered based on system requirements.

The convergence of memristors and transistors, particularly through the integration of 2D materials, is catalyzing significant advancements in in-memory computing, in-sensory systems⁹⁵, and neuromorphic computing¹³⁵. Memristors, which are known for their non-volatile resistance switching capabilities, combined with the high electron mobility and tunable electronic properties of 2D materials^{38,68}, are enabling the development of hybrid devices that offer enhanced functionality and performance. Transistor-memristor integration facilitates the creation of compact, energy-efficient circuits that are capable of both data storage and processing, reducing latency and power consumption in computing systems^{38,68,135,138,179,180}. In-sensory applications benefit from the ability of these hybrid devices to mimic biological synapses, resulting in more efficient and accurate sensory data processing⁹⁵. Additionally, the neuromorphic computing domain is witnessing transformative innovations because these integrated systems can emulate neural networks with greater precision, paving the way for advanced AI applications that closely replicate human cognitive functions.

Challenges and opportunities

Memristors constructed from 2D materials represent a rapidly evolving area with significant potential for a range of applications beyond conventional memory devices, similar to their traditional counterparts. Recent research has resulted in significant performance improvements by focusing on the synthesis of memristive arrays, which are critical for future computing systems^{88,135,181,182}. However, achieving high-performance memristive arrays poses significant challenges. One critical hurdle is the downsizing process. Reducing the thickness of these materials is essential for lowering the switching voltage of memristors, which in turn reduces energy consumption in low-power in-memory computing applications. However, ultra-thin 2D

materials often experience greater thickness variations, causing increased fluctuations in switching voltage. Additionally, thinner layers are more prone to forming wrinkles and microscale holes, which can significantly impact the effective thickness of the switching medium and result in short circuits, decreasing the yield. Minimizing device feature sizes is essential for constructing high-density memristor crossbar arrays, which are crucial for complex neural networks. However, as feature sizes shrink, the operating voltages could increase due to the challenges posed by the absence of defect paths or grain boundaries. This issue underscores the gap between current device capabilities and the requirements for integrating advanced CMOS technology^{135,182,183}.

Integrating memristors with access selectors or transistors to form extensive crossbar arrays introduces additional complexities, such as elevating the switching voltage and device latency, affecting energy efficiency and operational speed. For example, when selectors and transistors are activated, they function as resistors, requiring a higher voltage across the devices to have the same RS parameters as standalone memristors. Furthermore, the forming voltage of memristors based on 2D materials typically exceeds 1 V, limiting their compatibility with advanced CMOS transistors. Moreover, the difference between the reset current of memristors and the ON-state current of selectors or transistors requires larger areas for these components, which affects scalability. Another major challenge is ensuring the precise control of D2D variations and switching mechanisms within these arrays. Therefore, obtaining a high degree of controllability is essential, as variations in devices directly affect both yield and cost-effectiveness. This means that achieving reliable features in 2D-based memristors is difficult and demands precise control over the switching parameters and *I-V* characteristics.

There is a deficiency in clear quantitative models for certain switching behaviors, such as low retention time and high forming voltage. Identifying the key factors that contribute to device variations and developing effective control strategies can be achieved by combining experimental research with theoretical analyses and simulations. Training synapses remains a significant challenge with current technology. To enable systems to learn and adapt effectively, it is essential to achieve high accuracy and minimize programming errors, broadening the potential applications of neuromorphic computing. Recently developed crossbar arrays have mainly supported synapse inference and software-based training, with only a few efforts directed toward full-hardware online training. Obstacles such as C2C variations, discrepancies in writing and reading margins across devices, and endurance limitations hinder the achievement of high accuracy. These issues also constrain the feasibility of online training, highlighting the need for further research to develop reliable and efficient training mechanisms. Memristors also hold promise for applications in security devices and sensory computing, although these domains introduce additional challenges. In security devices, ensuring reliable and tamper-resistant data storage is paramount. Here, memristors' inherent non-volatility and potential for high-density integration make them an attractive proposition for secure data storage.

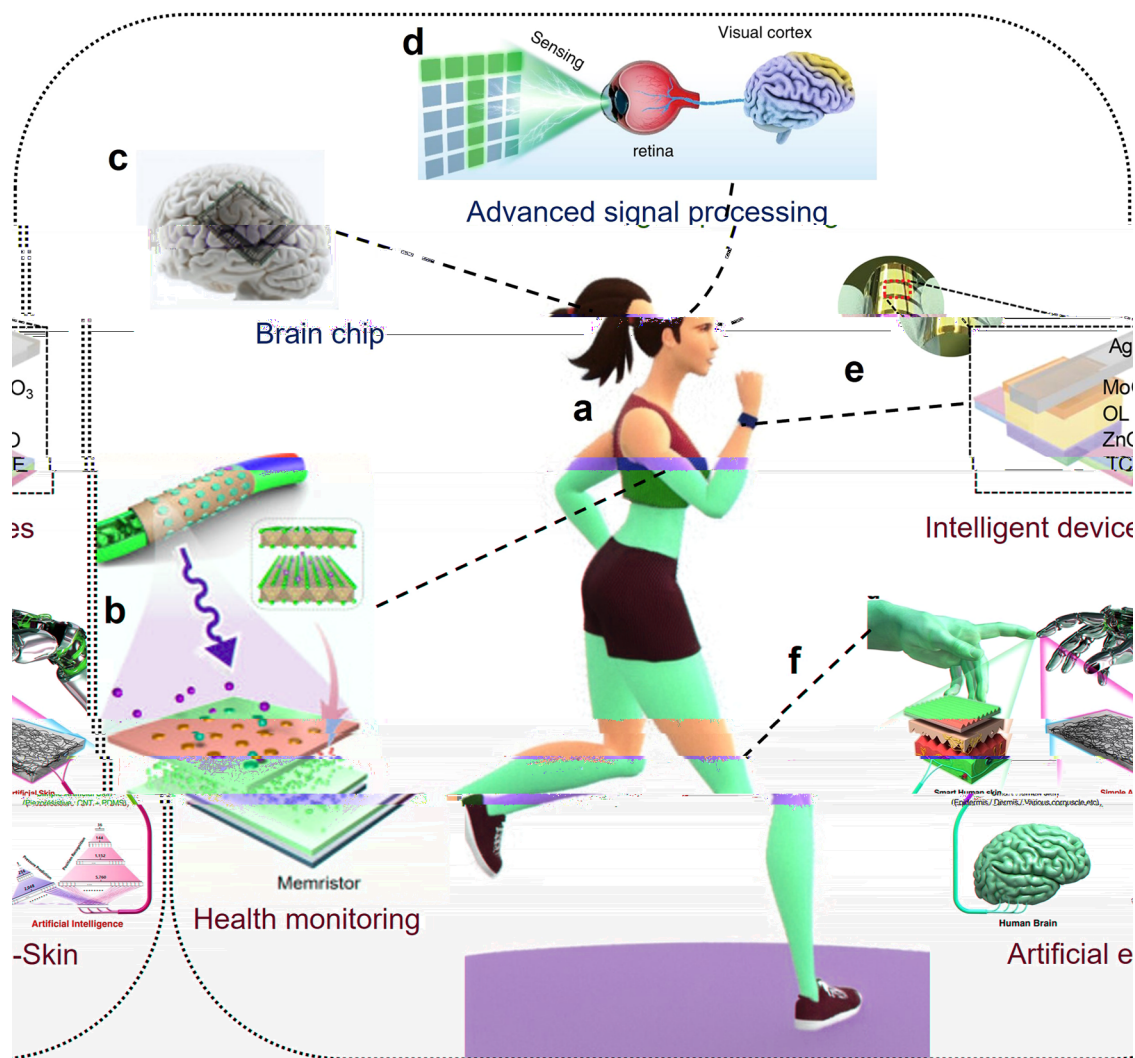


Fig. 10 | Future prospects of 2D layered materials-based memristors. a Human body image. Adapted from ref. 209. **b** Memristor for health monitoring. Reproduced with permission from ref. 210. **c** Brain chip. Reproduced with permission from ref. 62. **d** Human visual system for sensing, memory, and computing. Reproduced

with permission from ref. 211. **e** Intelligent devices applied to the wrist. Reproduced with permission from ref. 50. **f** Artificial skin. Reproduced with permission from ref. 212.

Unfortunately, the variability in switching behavior and the susceptibility of 2D materials to defects can result in vulnerabilities. Ensuring robust and repeatable switching characteristics is crucial to prevent unauthorized access and data corruption. In sensory computing, memristors can mimic synaptic functions, offering advantages for real-time data processing and low-power operation. Nonetheless, achieving consistent performance in diverse environmental conditions remains a challenge. For example, variations in temperature and humidity can affect the electrical properties of 2D materials, resulting in drift and reduced reliability in sensory applications. Therefore, developing materials and device architectures that maintain stable performance under varying conditions is essential for practical implementation. Furthermore, integrating memristors into complex sensory networks requires addressing issues related to signal-to-noise ratio and interference. The small size and high density of memristor arrays can worsen crosstalk and signal degradation, negatively affecting the accuracy of sensory data processing. Accordingly, advanced fabrication techniques and innovative circuit designs are required to minimize these effects and enhance the overall reliability and performance of memristor-based sensory systems. Continued research and development efforts are necessary to overcome these hurdles and fully realize the capabilities of 2D materials-based memristors in advanced computing systems.

Future prospective

The field of 2D layered material memristors is poised for significant advancements that extend their utility far beyond traditional memory applications. The performance of 2D layered materials-based memristors can be significantly enhanced by improving their speed, efficiency, durability, scalability, functionality, and application-specific optimizations. These advancements have the potential to unlock new capabilities and applications, resulting in innovative applications such as brain-like computing, communications, sensing, and health (Fig. 10a–f). To fully unleash the potential of 2D layered material memristors in device fabrication, ongoing interdisciplinary research and collaboration will be essential. This will involve integrating materials science, electrical engineering, computer science, and neuroscience insights. By overcoming current limitations and exploring new applications, 2D memristors could play a pivotal role in the future of various technologies. In terms of applications, although 2D materials have advanced neuromorphic systems and synaptic devices, brain-like computing remains in its nascent stages. However, the thinness and flexibility of 2D materials make memristors ideal for integration into flexible and wearable electronics. Future research will probably involve enhancing the mechanical durability and performance stability of these devices, enabling innovative applications in smart textiles, health monitoring devices, and flexible displays.

Moreover, the unique properties of 2D material memristors can also contribute to the development of ultra-low-power electronic devices, resulting in advancements in portable and battery-operated devices that will significantly extend their operational lifetimes and reduce energy consumption. Additionally, the quantum mechanical properties of 2D materials might be harnessed to develop quantum memristors, potentially revolutionizing quantum computing capabilities. Furthermore, 2D material memristors could be used in bioelectronic devices as an in-sensor computing device for real-time monitoring of biological processes and neural activity and targeted stimulation for therapeutic applications, offering new treatments for medical conditions. These memristors would also be suitable for environmental monitoring applications, with potential uses in pollution monitoring, climate change studies, and ecosystem management.

The integration of 2D material memristors into smart infrastructure systems presents another exciting avenue for development. Applications in smart grids, intelligent transportation systems, and building automation could enhance the monitoring and management of critical infrastructure, improving overall efficiency, safety, and sustainability. In addition, the integration of optoelectronics with memristor technology represents a promising frontier. By combining optical signals with electronic memristors, we can achieve significant gains in energy efficiency and expand the capabilities of these devices. This hybrid approach allows for faster data transmission and processing while also leveraging the advantages of light, such as high bandwidth and low energy loss. Optoelectronic memristors could facilitate advanced applications in neuromorphic computing, enabling real-time processing of large datasets and enhancing the performance of artificial intelligence and machine learning algorithms. As research progresses, developing materials and devices that effectively interface optical and electronic signals will be crucial. Innovations in 2D materials, such as transition metal dichalcogenides and other semiconductors, may provide the necessary properties for this integration. Ultimately, the convergence of optoelectronics and memristor technology holds the potential to revolutionize computing paradigms, paving the way for next-generation devices that are faster, more efficient, and capable of addressing complex tasks across various fields.

Conclusion

This review provides a detailed overview of the development roadmap of 2D material memristors and their expansion beyond memory applications. The practical application of memristor technology based on 2D layered materials remains in the early stages of exploration. 2D materials offer an efficient resistive switching mechanism based on the physical shape of the device. Switching mechanisms generally involve processes such as ion movement, phase changes, migration of vacancies, and the formation of conductive filaments. In the review, we systematically discussed the effective use of 2D layered materials-based memristors for neuromorphic computing, in-memory computing, in-sensor computing, and hardware security. This review can act as a guide for ongoing development and is anticipated to drive continuous breakthroughs and improvements in devices, architectures, and algorithms, contributing to the anticipated progress in memristor-based computing systems.

Data availability

The data that support the findings of this study are available from the corresponding author upon reasonable request.

Received: 25 August 2024; Accepted: 3 December 2024;

Published online: 21 December 2024

References

1. Chua, L. Memristor-the missing circuit element. *IEEE Trans. Circuit Theor.* **18**, 507–519 (1971).
2. Strukov, D. B., Snider, G. S., Stewart, D. R. & Williams, R. S. The missing memristor found. *Nature* **453**, 80–83 (2008).
3. Pickett, M. D., Medeiros-Ribeiro, G. & Williams, R. S. A scalable neuristor built with Mott memristors. *Nat. Mater.* **12**, 114–117 (2013).
4. Vlasov, A. I., Gudoshnikov, I. V., Zhalnin, V. P., Kadyr, A. T. & Shakhnov, V. A. Market for memristors and data mining memory structures for promising smart systems. *Entrep. Sustain. Issues* **8**, 98 (2020).
5. Batool, S., Idrees, M., Zhang, S.-R., Han, S.-T. & Zhou, Y. Novel charm of 2D materials engineering in memristor: when electronics encounter layered morphology. *Nanoscale Horiz.* **7**, 480–507 (2022).
6. Li, Y., Wang, Z., Midya, R., Xia, Q. & Yang, J. J. Review of memristor devices in neuromorphic computing: materials sciences and device challenges. *J. Phys. D Appl. Phys.* **51**, 503002 (2018).
7. Cao, Z. et al. Memristor-based neural networks: a bridge from device to artificial intelligence. *Nanoscale Horiz.* **8**, 716–745 (2023).
8. Xie, J., Afshari, S. & Sanchez Esqueda, I. Hexagonal boron nitride (h-BN) memristor arrays for analog-based machine learning hardware. *npj 2D Mater. Appl.* **6**, 1–7 (2022).
9. Gantz, J. & Reinsel, D. The Digital Universe In 2020: Big Data, Bigger Digital Shadows, and Biggest Growth in the Far East. in *Idc*. 1–16.
10. Gebregiorgis, A. et al. A survey on memory-centric computer architectures. *J. Emerg. Technol. Comput. Syst.* **18**, 1–50 (2022).
11. Hamdioui, S. et al. Memristor for computing: myth or reality? *Design Autom. Test Eur. Conf. Exhibition (DATE)*, 722–731 (2017).
12. Zhou, Y. *Advanced Memory Technology: Functional Materials and Devices* (Royal Society of Chemistry, 2023).
13. Park, S. W. et al. Phase-change heterostructure with HfTe₂ confinement sublayers for enhanced thermal efficiency and low-power operation through Joule heating localization. *J. Mater. Sci. Technol.* **204**, 104–114 (2025).
14. Zhang, Z. et al. Memory materials and devices: from concept to application. *InfoMat* **2**, 261–290 (2020).
15. Khot, A. C. et al. 2D Ti₃C₂T_x MXene-derived self-assembled 3D TiO₂ nanoflowers for nonvolatile memory and synaptic learning applications. *J. Mater. Sci. Technol.* **150**, 1–10 (2023).
16. Kundale, S. S. et al. Review of electrochemically synthesized resistive switching devices: memory storage, neuromorphic computing, and sensing applications. *Nanomater* **13**, 1879 (2023).
17. Dongale, T. D., Khot, A. C., Takaloo, A. V. & Kim, T. G. Facile synthesis of nickel cobaltite quasi-hexagonal nanosheets for multilevel resistive switching and synaptic learning applications. *NPG Asia Mater.* **13**, 1–12 (2021).
18. Kumar, S., Wang, X., Strachan, J. P., Yang, Y. & Lu, W. D. Dynamical memristors for higher-complexity neuromorphic computing. *Nat. Rev. Mater.* **7**, 575–591 (2022).
19. Pazos, S. et al. Solution-processed memristors: performance and reliability. *Nat. Rev. Mater.* **9**, 358–373 (2024).
20. Pham, V.-T., Volos, C. & Kapitaniak, T. Chapter 13—Memristor, mem-systems and neuromorphic applications: a review. in *Mem-Elements for Neuromorphic Circuits with Artificial Intelligence Applications* (eds Volos, C. & Pham, V.-T.) 265–285
21. Dongale, T. D., Khot, A. C., Takaloo, A. V., Son, K. R. & Kim, T. G. Multilevel resistive switching and synaptic plasticity of nanoparticulated cobaltite oxide memristive device. *J. Mater. Sci. Technol.* **78**, 81–91 (2021).
22. Yu, S. & Chen, P.-Y. Emerging memory technologies: recent trends and prospects. *IEEE Solid-State Circuits Mag.* **8**, 43–56 (2016).
23. Choi, S. et al. Low-power self-rectifying memristive artificial neural network for near internet-of-things sensor computing. *Adv. Electron. Mater.* **7**, 2100050 (2021).
24. Liu, C. et al. Two-dimensional materials for next-generation computing technologies. *Nat. Nanotechnol.* **15**, 545–557 (2020).
25. Zhang, C. et al. Recent progress on 2D materials-based artificial synapses. *Crit. Rev. Solid State Mater. Sci.* **47**, 665–690 (2022).
26. Zhao, H. et al. Atomically thin femtojoule memristive device. *Adv. Mater.* **29**, 1703232 (2017).

27. Wu, X. et al. Thinnest nonvolatile memory based on monolayer h-BN. *Adv. Mater.* **31**, 1806790 (2019).
28. Wang, S. et al. Networking retinomorph sensor with memristive crossbar for brain-inspired visual perception. *Natl. Sci. Rev.* **8**, nwa172 (2021).
29. Sangwan, V. K. et al. Multi-terminal memtransistors from polycrystalline monolayer molybdenum disulfide. *Nature* **554**, 500–504 (2018).
30. Bae, J., Won, J. & Shim, W. The rise of memtransistors for neuromorphic hardware and In-memory computing. *Nano Energy* **126**, 109646 (2024).
31. Yan, X., Qian, J. H., Sangwan, V. K. & Hersam, M. C. Progress and challenges for memtransistors in neuromorphic circuits and systems. *Adv. Mater.* **34**, 2108025 (2022).
32. Sun, L. et al. Self-selective van der Waals heterostructures for large scale memory array. *Nat. Commun.* **10**, 3161 (2019).
33. Wang, C.-Y. et al. Gate-tunable van der Waals heterostructure for reconfigurable neural network vision sensor. *Sci. Adv.* **6**, eaba6173 (2020).
34. Mennel, L. et al. Ultrafast machine vision with 2D material neural network image sensors. *Nature* **579**, 62–66 (2020).
35. Wali, A. & Das, S. Two-dimensional memtransistors for non-von Neumann computing: progress and challenges. *Adv. Funct. Mater.* **34**, 2308129 (2024).
36. Yang, Y. et al. Three-terminal memtransistors based on two-dimensional layered gallium selenide nanosheets for potential low-power electronics applications. *Nano Energy* **57**, 566–573 (2019).
37. Chen, L. et al. Ultrasensitive and robust two-dimensional indium selenide flexible electronics and sensors for human motion detection. *Nano Energy* **76**, 105020 (2020).
38. Sivan, M. et al. All WSe₂ 1T1R resistive RAM cell for future monolithic 3D embedded memory integration. *Nat. Commun.* **10**, 5201 (2019).
39. Teja Nibhanupudi, S. S. et al. Ultra-fast switching memristors based on two-dimensional materials. *Nat. Commun.* **15**, 2334 (2024).
40. Yu, S. Neuro-inspired computing with emerging nonvolatile memories. *Proc. IEEE* **106**, 260–285 (2018).
41. Tadayoni, M. et al. Modeling split-gate flash memory cell for advanced neuromorphic computing. In *2018 IEEE Int. Conf. Microelectron. Test Struct. (ICMTS)* 27–30 (2018).
42. Merrikh-Bayat, F. et al. High-performance mixed-signal neurocomputing with nanoscale floating-gate memory cell arrays. *IEEE Trans. Neural Netw. Learn. Syst.* **29**, 4782–4790 (2018).
43. Shouval, H. Z., Wang, S. S. & Wittenberg, G. M. Spike timing dependent plasticity: a consequence of more fundamental learning rules. *Front. Comput. Neurosci.* **4**, 19 (2010).
44. Kim, T. H. et al. Nanoparticle assemblies as memristors. *Nano Lett.* **9**, 2229–2233 (2009).
45. Rokade, K. A. et al. CogniFiber: harnessing biocompatible and biodegradable 1d collagen nanofibers for sustainable nonvolatile memory and synaptic learning applications. *Adv. Mater.* **36**, 2312484 (2024).
46. Park, Y. & Lee, J.-S. Metal halide perovskite-based memristors for emerging memory applications. *J. Phys. Chem. Lett.* **13**, 5638–5647 (2022).
47. John, R. A. et al. Halide perovskite memristors as flexible and reconfigurable physical unclonable functions. *Nat. Commun.* **12**, 3681 (2021).
48. Patel, M. et al. Hybrid perovskite-based flexible and stable memristor by complete solution process for neuromorphic computing. *Adv. Electron. Mater.* **9**, 2200908 (2023).
49. Chen, Y. et al. Polymer memristor for information storage and neuromorphic applications. *Mater. Horiz.* **1**, 489–506 (2014).
50. Nirmal, K. A. et al. Flexible memristive organic solar cell using multilayer 2D titanium carbide MXene electrodes. *Adv. Sci.* **10**, 2300433 (2023).
51. Pustake, S. O. et al. Anti-bacterial and transparent allantoin biomaterial-based biocomposite for non-volatile memory and brain-inspired computing applications. *Mater. Lett.* **330**, 133412 (2023).
52. Khot, A. C., Dongale, T. D., Park, J. H., Kesavan, A. V. & Kim, T. G. Ti₃C₂-based MXene oxide nanosheets for resistive memory and synaptic learning applications. *ACS Appl. Mater. Interfaces* **13**, 5216–5227 (2021).
53. Mullani, N. B. et al. Surface modification of a titanium carbide MXene memristor to enhance memory window and low-power operation. *Adv. Funct. Mater.* **33**, 2300343 (2023).
54. Khot, A. C. et al. Amorphous boron nitride memristive device for high-density memory and neuromorphic computing applications. *ACS Appl. Mater. Interfaces* **14**, 10546–10557 (2022).
55. Nirmal, K. A., Nhivekar, G. S., Khot, A. C., Dongale, T. D. & Kim, T. G. Unraveling the effect of the water content in the electrolyte on the resistive switching properties of self-assembled one-dimensional anodized TiO₂ nanotubes. *J. Phys. Chem. Lett.* **13**, 7870–7880 (2022).
56. Kumar, S. et al. Y₂O₃-based crossbar array for analog and neuromorphic computation. *IEEE Trans. Electron Devices* **70**, 473–477 (2023).
57. Kumar, D. et al. Highly efficient back-end-of-line compatible flexible Si-based optical memristive crossbar array for edge neuromorphic physiological signal processing and bionic machine vision. *Nano-Micro Lett.* **16**, 238 (2024).
58. Abbas, Y. et al. Structural engineering of tantalum oxide based memristor and its electrical switching responses using rapid thermal annealing. *J. Alloy. Compd.* **759**, 44–51 (2018).
59. Sokolov, A. S., Jeon, Y.-R., Kim, S., Ku, B. & Choi, C. Bio-realistic synaptic characteristics in the cone-shaped ZnO memristive device. *NPG Asia Mater.* **11**, 1–15 (2019).
60. Khot, A. C. et al. Self-assembled vapor-transport-deposited SnS nanoflake-based memory devices with synaptic learning properties. *Appl. Surf. Sci.* **648**, 158994 (2024).
61. Katkar, P. K. et al. Binder-free synthesis of nanostructured amorphous cobalt phosphate for resistive memory and artificial synaptic device applications. *ACS Appl. Electron. Mater.* **4**, 1852–1863 (2022).
62. Duan, X. et al. Memristor-based neuromorphic chips. *Adv. Mater.* **36**, 2310704 (2024).
63. Kundale, S. S. et al. Effects of switching layer morphology on resistive switching behavior: A case study of electrochemically synthesized mixed-phase copper oxide memristive devices. *Appl. Mater. Today* **27**, 101460 (2022).
64. Patil, A. R., Dongale, T. D., Kamat, R. K. & Rajpure, K. Y. Binary metal oxide-based resistive switching memory devices: A status review. *Mater. Today Commun.* **34**, 105356 (2023).
65. Ju, D., Kim, J. H. & Kim, S. Highly uniform resistive switching characteristics of Ti/TaO_x/ITO memristor devices for neuromorphic system. *J. Alloy. Compd.* **961**, 170920 (2023).
66. Kumbhar, D. D. et al. Exploring statistical approaches for accessing the reliability of Y₂O₃-based memristive devices. *Microelectron. Eng.* **288**, 112166 (2024).
67. Zeng, S., Liu, C. & Zhou, P. Transistor engineering based on 2D materials in the post-silicon era. *Nat. Rev. Electr. Eng.* **1**, 335–348 (2024).
68. Zhou, H., Li, S., Ang, K.-W. & Zhang, Y.-W. Recent advances in in-memory computing: exploring memristor and memristor arrays with 2D materials. *Nano-Micro Lett.* **16**, 121 (2024).
69. Chia, X. & Pumera, M. Characteristics and performance of two-dimensional materials for electrocatalysis. *Nat. Catal.* **1**, 909–921 (2018).
70. Zhao, Q. et al. Current status and prospects of memristors based on novel 2D materials. *Mater. Horiz.* **7**, 1495–1518 (2020).
71. Tian, H. et al. In situ tuning of switching window in a gate-controlled bilayer graphene-electrode resistive memory device. *Adv. Mater.* **27**, 7767–7774 (2015).

72. Rehman, M. M., Siddiqui, G. U., Doh, Y. H. & Choi, K. H. Highly flexible and electroforming free resistive switching behavior of tungsten disulfide flakes fabricated through advanced printing technology. *Semicond. Sci. Technol.* **32**, 095001 (2017).
73. Luo, S. et al. A synaptic memristor based on two-dimensional layered WSe₂ nanosheets with short- and long-term plasticity. *Nanoscale* **13**, 6654–6660 (2021).
74. Tang, K. et al. Electronic and photoelectronic memristors based on 2D materials. *Adv. Electron. Mater.* **8**, 2101099 (2022).
75. Zhou, Y. et al. Black phosphorus based multicolor light-modulated transparent memristor with enhanced resistive switching performance. *ACS Appl. Mater. Interfaces* **12**, 25108–25114 (2020).
76. Yu, T. et al. A low-power memristor based on 2H–MoTe₂ nanosheets with synaptic plasticity and arithmetic functions. *Mater. Today Nano* **19**, 100233 (2022).
77. Meng, J.-L. et al. Flexible boron nitride-based memristor for in situ digital and analogue neuromorphic computing applications. *Mater. Horiz.* **8**, 538–546 (2021).
78. Akinwande, D. et al. Graphene and two-dimensional materials for silicon technology. *Nature* **573**, 507–518 (2019).
79. Yin, S. et al. Emulation of learning and memory behaviors by memristor based on ag migration on 2D MoS₂ surface. *Phys. Status Solidi (a)* **216**, 1900104 (2019).
80. Li, S. et al. Wafer-scale 2D hafnium diselenide based memristor crossbar array for energy-efficient neural network hardware. *Adv. Mater.* **34**, 2103376 (2022).
81. Yuan, B. et al. 150 nm × 200 nm cross-point hexagonal boron nitride-based memristors. *Adv. Electron. Mater.* **6**, 1900115 (2020).
82. He, N. et al. Influence of a novel 2D material MXene on the behavior of memristor and its crossbar array. *IEEE Intl. Conf. Electron Devices Solid-State Circuits (EDSSC)* 1–3 (2019).
83. Duan, H. et al. Low-power memristor based on two-dimensional materials. *J. Phys. Chem. Lett.* **13**, 7130–7138 (2022).
84. Yu, T. et al. MoTe₂-based low energy consumption artificial synapse for neuromorphic behavior and decimal arithmetic. *Mater. Today Chem.* **27**, 101268 (2023).
85. Feng, X. et al. A fully printed flexible MoS₂ memristive artificial synapse with femtojoule switching energy. *Adv. Electron. Mater.* **5**, 1900740 (2019).
86. Yan, X. et al. Robust Ag/ZrO₂/WS₂/Pt memristor for neuromorphic computing. *ACS Appl. Mater. Interfaces* **11**, 48029–48038 (2019).
87. Sokolov, A. et al. Partially oxidized MXene Ti₃C₂T_x sheets for memristor having synapse and threshold resistive switching characteristics. *Adv. Electron. Mater.* **7**, 2000866 (2021).
88. Wang, M. et al. Robust memristors based on layered two-dimensional materials. *Nat. Electron* **1**, 130–136 (2018).
89. Gao, G. et al. Charge mediated semiconducting-to-metallic phase transition in molybdenum disulfide monolayer and hydrogen evolution reaction in new 1T' phase. *J. Phys. Chem. C* **119**, 13124–13128 (2015).
90. Zhang, F. et al. Electric-field induced structural transition in vertical MoTe₂- and Mo1-xWxTe₂-based resistive memories. *Nat. Mater.* **18**, 55–61 (2019).
91. Hou, W. et al. Strain engineering of vertical molybdenum ditelluride phase-change memristors. *Nat. Electron.* **7**, 8–16 (2024).
92. Lei, X. et al. Nonvolatile and volatile resistive switching characteristics in MoS₂ thin film for RRAM application. *J. Alloy. Compd.* **969**, 172443 (2023).
93. Seo, S. et al. Artificial optic-neural synapse for colored and color-mixed pattern recognition. *Nat. Commun.* **9**, 5106 (2018).
94. Lv, S., Liu, J. & Geng, Z. Application of memristors in hardware security: a current state-of-the-art technology. *Adv. Intell. Syst.* **3**, 2000127 (2021).
95. Sun, L. et al. In-sensor reservoir computing for language learning via two-dimensional memristors. *Sci. Adv.* **7**, eabg1455 (2021).
96. Pi, S., Ghadiri-Sadrabadi, M., Bardin, J. C. & Xia, Q. Memristors as radiofrequency switches. *IEEE Intl. Symp. Circuits Syst. (ISCAS)* 377–380 (2016).
97. Huh, W., Lee, D. & Lee, C.-H. Memristors based on 2D materials as an artificial synapse for neuromorphic electronics. *Adv. Mater.* **32**, 2002092 (2020).
98. Wang, K., Chen, J. & Yan, X. MXene Ti₃C₂ memristor for neuromorphic behavior and decimal arithmetic operation applications. *Nano Energy* **79**, 105453 (2021).
99. Wang, S., Zhang, D. W. & Zhou, P. Two-dimensional materials for synaptic electronics and neuromorphic systems. *Sci. Bull.* **64**, 1056–1066 (2019).
100. Li, C. et al. Short-term synaptic plasticity in emerging devices for neuromorphic computing. *iSci* **26**, 106315 (2023).
101. Jana, R., Ghosh, S., Bhunia, R. & Chowdhury, A. Recent developments in the state-of-the-art optoelectronic synaptic devices based on 2D materials: a review. *J. Mater. Chem. C* **12**, 5299–5338 (2024).
102. Yan, X. et al. Vacancy-induced synaptic behavior in 2D WS₂ nanosheet-based memristor for low-power neuromorphic computing. *Small* **15**, 1901423 (2019).
103. Tang, B. et al. Wafer-scale solution-processed 2D material analog resistive memory array for memory-based computing. *Nat. Commun.* **13**, 3037 (2022).
104. Khot, A. C., Nirmal, K. A., Dongale, T. D. & Kim, T. G. GeTe/MoTe₂ van der Waals heterostructures: enabling ultralow voltage memristors for nonvolatile memory and neuromorphic computing applications. *Small* **20**, 2400791 (2024).
105. Afshari, S., Xie, J., Musisi-Nkambwe, M., Radhakrishnan, S. & Sanchez Esqueda, I. Unsupervised learning in hexagonal boron nitride memristor-based spiking neural networks. *Nanotechnol* **34**, 445703 (2023).
106. Li, Y. et al. In-memory computing using memristor arrays with ultrathin 2D PdSeO/PdSe₂ heterostructure. *Adv. Mater.* **34**, 2201488 (2022).
107. Hao, S. et al. A monolayer leaky integrate-and-fire neuron for 2D memristive neuromorphic networks. *Adv. Electron. Mater.* **6**, 1901335 (2020).
108. Feng, X. et al. Self-selective multi-terminal memtransistor crossbar array for in-memory computing. *ACS Nano* **15**, 1764–1774 (2021).
109. Yang, J.-Q. et al. Leaky integrate-and-fire neurons based on perovskite memristor for spiking neural networks. *Nano Energy* **74**, 104828 (2020).
110. Yi, W. et al. Biological plausibility and stochasticity in scalable VO₂ active memristor neurons. *Nat. Commun.* **9**, 4661 (2018).
111. Tuma, T., Pantazi, A., Le Gallo, M., Sebastian, A. & Eleftheriou, E. Stochastic phase-change neurons. *Nat. Nanotech.* **11**, 693–699 (2016).
112. Bousoulas, P., Panagopoulou, M., Boukos, N. & Tsoukalas, D. Emulating artificial neuron and synaptic properties with SiO₂-based memristive devices by tuning threshold and bipolar switching effects. *J. Phys. D Appl. Phys.* **54**, 225303 (2021).
113. Roldan, J. B. et al. Spiking neural networks based on two-dimensional materials. *npj 2D Mater. Appl.* **6**, 1–7 (2022).
114. Ma, S. et al. An artificial neural network chip based on two-dimensional semiconductor. *Sci. Bull.* **67**, 270–277 (2022).
115. Lu, X. F. et al. Exploring low power and ultrafast memristor on p-type van der waals sns. *Nano Lett.* **21**, 8800–8807 (2021).
116. Yao, P. et al. Fully hardware-implemented memristor convolutional neural network. *Nature* **577**, 641–646 (2020).
117. Fatima, S., Bin, X., Mohammad, M. A., Akinwande, D. & Rizwan, S. Graphene and MXene based free-standing carbon memristors for flexible 2D memory applications. *Adv. Electron. Mater.* **8**, 2100549 (2022).
118. Vu, Q. A. et al. A High-on/off-ratio floating-gate memristor array on a flexible substrate via CVD-grown large-area 2D layer stacking. *Adv. Mater.* **29**, 1703363 (2017).

119. Tian, H. et al. Monitoring oxygen movement by Raman spectroscopy of resistive random access memory with a graphene-inserted electrode. *Nano Lett.* **13**, 651–657 (2013).
120. Baeumer, C. et al. Quantifying redox-induced Schottky barrier variations in memristive devices via in operando spectromicroscopy with graphene electrodes. *Nat. Commun.* **7**, 12398 (2016).
121. Ahn, C. et al. Energy-efficient phase-change memory with graphene as a thermal barrier. *Nano Lett.* **15**, 6809–6814 (2015).
122. Krishnaprasad, A. et al. Electronic synapses with near-linear weight update using MoS₂/graphene memristors. *Appl. Phys. Lett.* **115**, 103104 (2019).
123. Pan, C. et al. Coexistence of grain-boundaries-assisted bipolar and threshold resistive switching in multilayer hexagonal boron nitride. *Adv. Funct. Mater.* **27**, 1604811 (2017).
124. Kumar, M., Ban, D.-K., Kim, S. M., Kim, J. & Wong, C.-P. Vertically aligned WS₂ layers for high-performing memristors and artificial synapses. *Adv. Electron. Mater.* **5**, 1900467 (2019).
125. Zhu, K. et al. Graphene–Boron Nitride–Graphene cross-point memristors with three stable resistive states. *ACS Appl. Mater. Interfaces* **11**, 37999–38005 (2019).
126. Xu, R. et al. Vertical MoS₂ double-layer memristor with electrochemical metallization as an atomic-scale synapse with switching thresholds approaching 100 mV. *Nano Lett.* **19**, 2411–2417 (2019).
127. Wang, K. et al. A pure 2H-MoS₂ nanosheet-based memristor with low power consumption and linear multilevel storage for artificial synapse emulator. *Adv. Electron. Mater.* **6**, 1901342 (2020).
128. Musisi-Nkambwe, M., Afshari, S., Xie, J., Warner, H. & Sanchez Esqueda, I. A study on h-BN resistive switching temporal response. *Adv. Electron. Mater.* **10**, 2400022 (2024).
129. Cao, G. et al. 2D material based synaptic devices for neuromorphic computing. *Adv. Funct. Mater.* **31**, 2005443 (2021).
130. Sangwan, V. K. & Hersam, M. C. Neuromorphic nanoelectronic materials. *Nat. Nanotechnol.* **15**, 517–528 (2020).
131. Tseng, P.-T. et al. Peripheral iron levels in children with attention-deficit hyperactivity disorder: a systematic review and meta-analysis. *Sci. Rep.* **8**, 788 (2018).
132. Zhang, W. et al. Neuro-inspired computing chips. *Nat. Electron.* **3**, 371–382 (2020).
133. Li, Y. et al. Anomalous resistive switching in memristors based on two-dimensional palladium diselenide using heterophase grain boundaries. *Nat. Electron.* **4**, 348–356 (2021).
134. Shi, Y. et al. Electronic synapses made of layered two-dimensional materials. *Nat. Electron.* **1**, 458–465 (2018).
135. Zhu, K. et al. Hybrid 2D–CMOS microchips for memristive applications. *Nature* **618**, 57–62 (2023).
136. Yeh, C.-H., Zhang, D., Cao, W. & Banerjee, K. 0.5T0.5R - Introducing an ultra-compact memory cell enabled by shared graphene edge-contact and h-BN insulator. *IEEE Intl. Electron Devices Meeting (IEDM)* 12.3.1–12.3.4 (2020).
137. Li, Y. & Ang, K.-W. Hardware implementation of neuromorphic computing using large-scale memristor crossbar arrays. *Adv. Intel. Syst.* **3**, 2000137 (2021).
138. Lee, H.-S. et al. Dual-gated MoS₂ memristor crossbar array. *Adv. Funct. Mater.* **30**, 2003683 (2020).
139. Chen, S. et al. Wafer-scale integration of two-dimensional materials in high-density memristive crossbar arrays for artificial neural networks. *Nat. Electron.* **3**, 638–645 (2020).
140. Naqi, M. et al. Multilevel artificial electronic synaptic device of direct grown robust MoS₂ based memristor array for in-memory deep neural network. *npj 2D Mater. Appl.* **6**, 1–9 (2022).
141. Zhang, Z. et al. 2D materials and van der Waals heterojunctions for neuromorphic computing. *Neuromorph. Comput. Eng.* **2**, 032004 (2022).
142. Finateu, T. et al. 5.10 A 1280 × 720 Back-illuminated stacked temporal contrast event-based vision sensor with 4.86µm pixels, 1.066geps readout, programmable event-rate controller and compressive data-formatting pipeline. *IEEE Intl. Solid-State Circuits Conf. - (ISSCC)* 112–114 (2020).
143. Shulaker, M. M. et al. Three-dimensional integration of nanotechnologies for computing and data storage on a single chip. *Nature* **547**, 74–78 (2017).
144. Zhou, F. & Chai, Y. Near-sensor and in-sensor computing. *Nat. Electron.* **3**, 664–671 (2020).
145. Wu, T.-Y. et al. Sub-nA low-current HZO ferroelectric tunnel junction for high-performance and accurate deep learning acceleration. *IEEE Intl. Electron Devices Meeting (IEDM)* 6.3.1–6.3.4 (2019).
146. Tang, K.-T. et al. Considerations of integrating computing-in-memory and processing-in-sensor into convolutional neural network accelerators for low-power edge devices. *Symp. VLSI Circuits* T166–T167 (2019).
147. Lin, Y. et al. Multifunctional optoelectronic memristor based on CeO₂/MoS₂ heterojunction for advanced artificial synapses and bionic visual system with nociceptive sensing. *Nano Energy* **121**, 109267 (2024).
148. Dutta, T. et al. Electronic properties of 2D materials and their junctions. *Nano Mater. Sci.* **6**, 1–23 (2024).
149. Ng, L. W. T. et al. Structures, properties and applications of 2D materials. *Printing of Graphene and Related 2D Materials: Technology, Formulation and Applications* (eds Ng, L. W. T. et al.) 19–51 (Springer International Publishing, 2019).
150. Hayat, A. et al. Recent advances, properties, fabrication and opportunities in two-dimensional materials for their potential sustainable applications. *Energy Storage Mater.* **59**, 102780 (2023).
151. Zhang, W. et al. An ultrathin memristor based on a two-dimensional WS₂/MoS₂ heterojunction. *Nanoscale* **13**, 11497–11504 (2021).
152. Kundale, S. S. et al. Multilevel conductance states of vapor-transport-deposited Sb₂S₃ memristors achieved via electrical and optical modulation. *Adv. Sci.* **11**, 2405251 (2024).
153. Moon, G. et al. Atomically thin synapse networks on van der Waals photo-memtransistors. *Adv. Mater.* **35**, 2203481 (2023).
154. Tong, L. et al. 2D materials–based homogeneous transistor-memory architecture for neuromorphic hardware. *Sci* **373**, 1353–1358 (2021).
155. Sebastian, A. et al. Two-dimensional materials-based probabilistic synapses and reconfigurable neurons for measuring inference uncertainty using Bayesian neural networks. *Nat. Commun.* **13**, 6139 (2022).
156. Nili, H. et al. Hardware-intrinsic security primitives enabled by analogue state and nonlinear conductance variations in integrated memristors. *Nat. Electron.* **1**, 197–202 (2018).
157. Chen, A. Reconfigurable physical unclonable function based on probabilistic switching of RRAM. *Electron. Lett.* **51**, 615–617 (2015).
158. Pang, Y. et al. Optimization of RRAM-based physical unclonable function with a novel differential read-out method. *IEEE Electron Device Lett.* **38**, 168–171 (2017).
159. Lillis, W., HOFFING, M. C. & Burleson, W. Survey of security issues in memristor-based machine learning accelerators for RF analysis. *Chips* **3**, 196–215 (2024).
160. Cambou, B. F. Design of true random numbers generators with ternary physical unclonable functions. *Adv. Sci. Technol. Eng. Syst.* **3**, 15–29 (2018).
161. Woo, K. S. et al. Tunable stochastic memristors for energy-efficient encryption and computing. *Nat. Commun.* **15**, 3245 (2024).
162. Chen, A. Utilizing the variability of resistive random access memory to implement reconfigurable physical unclonable functions. *IEEE Electron Device Lett.* **36**, 138–140 (2015).
163. Gao, L., Chen, P.-Y., Liu, R. & Yu, S. Physical unclonable function exploiting sneak paths in resistive cross-point array. *IEEE Trans. Electron Devices* **63**, 3109–3115 (2016).
164. Mathew, J., Chakraborty, R. S., Sahoo, D. P., Yang, Y. & Pradhan, D. K. A novel memristor based physically unclonable function. *Integr. VLSI J.* **51**, 37–45 (2015).

165. Gao, Y., Ranasinghe, D. C., Al-Sarawi, S. F., Kavehei, O. & Abbott, D. Emerging physical unclonable functions with nanotechnology. *IEEE Access* **4**, 61–80 (2016).
166. Gao, Y., Ranasinghe, D. C., Al-Sarawi, S. F., Kavehei, O. & Abbott, D. Memristive crypto primitive for building highly secure physical unclonable functions. *Sci. Rep.* **5**, 12785 (2015).
167. Huang, C.-Y., Shen, W. C., Tseng, Y.-H., King, Y.-C. & Lin, C.-J. A Contact-resistive random-access-memory-based true random number generator. *IEEE Electron Device Lett.* **33**, 1108–1110 (2012).
168. Dodda, A., Trainor, N., Redwing, J. M. & Das, S. All-in-one, bio-inspired, and low-power crypto engines for near-sensor security based on two-dimensional memtransistors. *Nat. Commun.* **13**, 3587 (2022).
169. Pazos, S. et al. Hardware implementation of a true random number generator integrating a hexagonal boron nitride memristor with a commercial microcontroller. *Nanoscale* **15**, 2171–2180 (2023).
170. Wen, C. et al. Advanced data encryption using 2D materials. *Adv. Mater.* **33**, 2100185 (2021).
171. Balatti, S. et al. Physical unbiased generation of random numbers with coupled resistive switching devices. *IEEE Trans. Electron Devices* **63**, 2029–2035 (2016).
172. Carboni, R. et al. Random number generation by differential read of stochastic switching in spin-transfer torque memory. *IEEE Electron Device Lett.* **39**, 951–954 (2018).
173. Go, S.-X., Lim, K.-G., Lee, T.-H. & Loke, D. K. Nonvolatile memristive materials and physical modeling for in-memory and in-sensor computing. *Small Sci.* **4**, 2300139 (2024).
174. Sahay, S., Suri, M., Kumar, A. & Parmar, V. Hybrid CMOS-OxRAM RNG circuits. *IEEE 16th Intl. Conf. Nanotechnol. (IEEE-NANO)* 393–396 (2016).
175. Kim, J. et al. Nano-intrinsic true random number generation: A device to data study. *IEEE Trans. Circuits Syst.* **66**, 2615–2626 (2019).
176. Sahay, S., Kumar, A., Parmar, V. & Suri, M. OxRAM RNG circuits exploiting multiple undesirable nanoscale phenomena. *IEEE Trans. Nanotechnol.* **16**, 560–566 (2017).
177. Fischer, V., Bernard, F., Bochar, N. & Varchola, M. Enhancing security of ring oscillator-based trng implemented in FPGA. in *2008 Intl. Conf. Field Programmable Logic Appl.* 245–250 (2008).
178. Wali, A., Ravichandran, H. & Das, S. A Machine learning attack resilient true random number generator based on stochastic programming of atomically thin transistors. *ACS Nano* **15**, 17804–17812 (2021).
179. Wang, L. et al. Artificial synapses based on multiterminal memtransistors for neuromorphic application. *Adv. Funct. Mater.* **29**, 1901106 (2019).
180. Yin, L. et al. Two-dimensional unipolar memristors with logic and memory functions. *Nano Lett.* **20**, 4144–4152 (2020).
181. Kwon, K. C., Baek, J. H., Hong, K., Kim, S. Y. & Jang, H. W. Memristive devices based on two-dimensional transition metal chalcogenides for neuromorphic computing. *Nano-Micro Lett.* **14**, 58 (2022).
182. Lanza, M. et al. Memristive technologies for data storage, computation, encryption, and radio-frequency communication. *Science* **376**, eabj9979 (2022).
183. Lanza, M., Molas, G. & Naveh, I. The gap between academia and industry in resistive switching research. *Nat. Electron.* **6**, 260–263 (2023).
184. Sangwan, V. K. et al. Gate-tunable memristive phenomena mediated by grain boundaries in single-layer MoS₂. *Nat. Nanotech.* **10**, 403–406 (2015).
185. Duan, H. et al. Memristors based on 2D MoSe₂ nanosheets as artificial synapses and nociceptors for neuromorphic computing. *Nanoscale* **15**, 10089–10096 (2023).
186. Jeon, Y.-R. et al. Suppressed stochastic switching behavior and improved synaptic functions in an atomic switch embedded with a 2D NbSe₂ material. *ACS Appl. Mater. Interfaces* **13**, 10161–10170 (2021).
187. Zhong, L., Xie, W., Yin, J. & Jie, W. Chemical-vapor-deposited 2D VSe₂ nanosheet with threshold switching behaviors for Boolean logic calculations and leaky integrate-and-fire functions. *J. Mater. Chem. C* **11**, 5032–5038 (2023).
188. Qin, Y. et al. Threshold switching memristor based on 2D SnSe for nociceptive and leaky-integrate and fire neuron simulation. *ACS Appl. Electron. Mater.* **6**, 4939–4947 (2024).
189. Tang, J. et al. The degradation mechanism and stability enhancement of GaSe lateral memristors. *Appl. Phys. Lett.* **124**, 123102 (2024).
190. Yu, M. J. et al. Three Musketeers: demonstration of multilevel memory, selector, and synaptic behaviors from an Ag-GeTe based chalcogenide material. *J. Mater. Res. Technol.* **15**, 1984–1995 (2021).
191. Huang, Y. et al. ReSe₂-based RRAM and circuit-level model for neuromorphic computing. *Front. Nanotechnol.* **3**, 782836 (2021).
192. Wang, Z. et al. Superlow power consumption artificial synapses based on WSe₂ quantum dots memristor for neuromorphic computing. *Research* **2022**, 13 (2022).
193. Tian, H. et al. Extremely low operating current resistive memory based on exfoliated 2D perovskite single crystals for neuromorphic computing. *ACS Nano* **11**, 12247–12256 (2017).
194. Xiao, Y. et al. 2D MoTe₂/MoS_{2-x}O_x van der Waals heterostructure for bimodal neuromorphic optoelectronic computing. *Adv. Electron. Mater.* **9**, 2300388 (2023).
195. Bessonov, A. A. et al. Layered memristive and memcapacitive switches for printable electronics. *Nat. Mater.* **14**, 199–204 (2015).
196. Huh, W. et al. Synaptic barristor based on phase-engineered 2D heterostructures. *Adv. Mater.* **30**, 1801447 (2018).
197. Wang, Z. et al. Memristors with diffusive dynamics as synaptic emulators for neuromorphic computing. *Nat. Mater.* **16**, 101–108 (2017).
198. Tian, H. et al. A novel artificial synapse with dual modes using bilayer graphene as the bottom electrode. *Nanoscale* **9**, 9275–9283 (2017).
199. Zhang, Z. et al. Truly concomitant and independently expressed short-and long-term plasticity in a Bi₂O₂Se-based three-terminal memristor. *Adv. Mater.* **31**, 1805769 (2019).
200. Zhai, Y. et al. Infrared-sensitive memory based on direct-grown MoS₂-Upconversion-Nanoparticle Heterostructure. *Adv. Mater.* **30**, 1803563 (2018).
201. Wang, M. et al. A selector device based on graphene-oxide heterostructures for memristor crossbar applications. *Appl. Phys. A* **120**, 403–407 (2015).
202. Wang, C.-H. et al. 3D monolithic stacked 1T1R cells using monolayer MoS₂ FET and hBN RRAM fabricated at low (150 °C) temperature. in *2018 IEEE International Electron Devices Meeting (IEDM)* 22.5.1–22.5.4 (2018).
203. Li, D. et al. MoS₂ memristors exhibiting variable switching characteristics toward biorealistic synaptic emulation. *ACS Nano* **12**, 9240–9252 (2018).
204. Lin, Y. et al. Analog-digital hybrid memristive devices for image pattern recognition with tunable learning accuracy and speed. *Small Methods* **3**, 1900160 (2019).
205. Zhu, X., Li, D., Liang, X. & Lu, W. D. Ionic modulation and ionic coupling effects in MoS₂ devices for neuromorphic computing. *Nat. Mater.* **18**, 141–148 (2019).
206. Tian, H. et al. A hardware Markov chain algorithm realized in a single device for machine learning. *Nat. Commun.* **9**, 4305 (2018).
207. Xie, X., Kang, J., Gong, Y., Ajayan, P. M. & Banerjee, K. Room temperature 2D memristive transistor with optical short-term plasticity. In *2017 IEEE International Electron Devices Meeting (IEDM)* 5.3.1–5.3.4 (2017).

208. Tran, M. D. et al. Two-terminal multibit optical memory via van der Waals heterostructure. *Adv. Mater.* **31**, 1807075 (2019).
209. Zhang, J. et al. Memristor based electronic devices towards biomedical applications. *J. Mater. Chem. C* **12**, 50–59 (2024).
210. Cao, Z. et al. A reversible implantable memristor for health monitoring applications. *Mater. Today Bio.* **26**, 101096 (2024).
211. Fu, X. et al. Graphene/MoS_{2-x}O_x/graphene photomemristor with tunable non-volatile responsivities for neuromorphic vision processing. *Light Sci. Appl.* **12**, 39 (2023).
212. Sohn, K.-S. et al. An extremely simple macroscale electronic skin realized by deep machine learning. *Sci. Rep.* **7**, 11061 (2017).

Acknowledgements

This work was supported by a National Research Foundation of Korea (NRF) grant funded by the Korean Government (No. RS-2024-00407199, 2016R1A3B1908249). This work is dedicated to Prof. Pramod S. Patil, in recognition of his outstanding research in the field of Nanoscience and to commemorate his official superannuation from the Department of Physics, Shivaji University, Kolhapur, India.

Author contributions

T.G.K. and T.D.D. directed and supervised the project; K.A.N. and D.D.K. drafted the manuscript; T.D.D., A.V.K., and T.G.K. contributed to the review and editing; All authors contributed to the discussion and revision of the manuscript at all stages.

Competing interests

The author declares no competing interests.

Additional information

Correspondence and requests for materials should be addressed to Tukaram D. Dongale or Tae Geun Kim.

Reprints and permissions information is available at <http://www.nature.com/reprints>

Publisher's note Springer Nature remains neutral with regard to jurisdictional claims in published maps and institutional affiliations.

Open Access This article is licensed under a Creative Commons Attribution-NonCommercial-NoDerivatives 4.0 International License, which permits any non-commercial use, sharing, distribution and reproduction in any medium or format, as long as you give appropriate credit to the original author(s) and the source, provide a link to the Creative Commons licence, and indicate if you modified the licensed material. You do not have permission under this licence to share adapted material derived from this article or parts of it. The images or other third party material in this article are included in the article's Creative Commons licence, unless indicated otherwise in a credit line to the material. If material is not included in the article's Creative Commons licence and your intended use is not permitted by statutory regulation or exceeds the permitted use, you will need to obtain permission directly from the copyright holder. To view a copy of this licence, visit <http://creativecommons.org/licenses/by-nc-nd/4.0/>.

© The Author(s) 2024